

Radiation Boundary Conditions for Acoustic and Elastic Wave Calculations*

BJORN ENGQUIST

University of California

at

Los Angeles

AND

ANDREW MAJDA

University of California

at

Berkeley

0. Introduction

Because of the restrictions imposed by present day computers, many of the calculations in scientific computing require the use of artificial computational boundaries. This problem has stimulated considerable interest recently in the computational literature (see the bibliography in [4], [5] and [9]). Important areas of application which use artificial boundaries are seismology utilizing both scalar and elastic waves (see [1] and [5]), local and global numerical weather prediction (see [3] and [9]), and a wide variety of problems in transonic fluid dynamics.

In situations where the computed solution approximates a steady solution which possesses a regular far field asymptotic expansion, coordinate transformations are a traditional and an effective way to eliminate the difficulties with computational boundaries. This is certainly the case for many of the steady state problems in transonic flow. On the other hand, when highly oscillatory transient solutions are computed or when the computed solution has an asymptotic expansion with essential singularities near infinity, coordinate mapping techniques are ineffective and alternate approaches must be developed for treating the computational boundaries. These circumstances are typical for most calculations in seismology and some of the calculations in unsteady transonic flow and meteorology.

* The work of the first author was partially supported by the Swedish Natural Science Research Council (NFR 2711-018) and the second author was partially supported by the National Science Foundation under Grant No. NSF MCS 76-10227. This paper was presented at the Courant Institute of Mathematical Sciences Conference on Scientific Computing, April 20-22, 1977, held to inaugurate the Courant Professorship of Mathematical Sciences. Reproduction in whole or in part is permitted for any purpose of the United States Government.

In a recent paper (see [4]), the authors sketched a theory for developing hierarchies of radiating boundary conditions to be used at the artificial boundaries for the highly oscillatory and/or singular problems mentioned above. This hierarchy was designed to have the following three attractive computational features:

- (i) The boundary conditions substantially reduced the (unphysical) reflections from the artificial boundaries.
- (ii) The boundary conditions were local.
- (iii) The boundary conditions together with the interior differential equation defined a well-posed problem.

The strategy used in developing this hierarchy proceeded in three steps:

(a) First a theoretical reflectionless radiating boundary condition was developed at the artificial boundaries. For constant coefficient problems in planar geometries this theoretical radiating boundary condition could be written down exactly, while, for variable coefficient equations in general geometries, the theory of pseudo-differential operators and the reflection of singularities (see [7], [8], and Appendix A) allowed one to compute these boundary conditions at least asymptotically at large frequencies. Unfortunately, except in the most trivial one-dimensional cases, these boundary conditions are nonlocal simultaneously in space and time and are useless for practical problems.

(b) The next step was to approximate in a judicious fashion this nonlocal boundary condition by practical local and well-posed radiating boundary conditions which while not “reflectionless” did substantially reduce reflections at computational boundaries.

(c) Finally, these continuous radiating boundary conditions were approximated by discrete radiating boundary conditions which were then coupled to a standard interior discretization of the differential equation.

The test calculations in [4] for the constant coefficient scalar wave equation and the linearized shallow water equations strongly support the effectiveness of the strategy described above.

The objective of this paper is to develop further many of the theoretical and practical aspects of the basic method outlined in [4]. For simplicity we concentrate on a class of problems typical in exploration seismology using the acoustic or elastic wave equations. These calculations (see [5]) usually involve a rectangular region given by Figure 0.1, where $x=0$ is the surface of the earth with its layer structure below and the boundary $x=0$ is a physical boundary while the remaining three sides of the rectangle are computational artificial boundaries. One is interested in computing a solution which is a response to a known forcing function on the surface $x=0$, where this solution satisfies the variable coefficient acoustic or elastic wave equation with the

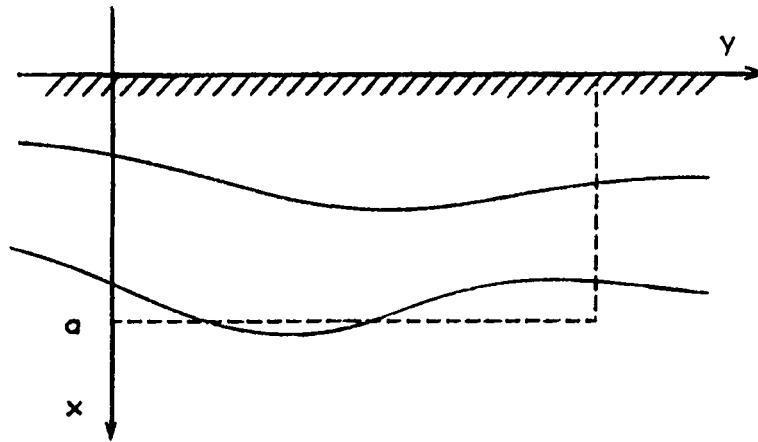


Figure 0.1. Earth model with rectangular computational boundaries.

appropriate physical boundary conditions at $x=0$. Below we shall analyze several theoretical and practical aspects of implementing the methods of [4] in this problem.

In Section 1, we consider the simplest version of the problem described in connection with Figure 0.1 and give a rigorous theoretical justification for the fact that the strategy sketched in (a) and (b) above must necessarily succeed. We consider the constant coefficient scalar wave equation where the artificial boundary in Figure 0.1 occurs at $x=a$ and by using continued fraction expansions we describe how to develop a systematic sequence of stable highly absorbing boundary conditions with successively better absorbing properties as the order of the boundary conditions increases. In Section 2, in a special example, we give a rigorous quantitative asymptotic comparison of various possible constant versus variable coefficient strategies for developing radiating boundary conditions in variable velocity media. In Section 3, we present a systematic derivation of a hierarchy of local radiating boundary conditions for the elastic wave equation. This derivation supplements the practical calculations for the elastic wave equation reported by Clayton and Engquist in [2] where radiating boundary conditions were used, successfully applying the methods in [4]. This derivation also has independent interest when “paraxial approximations” are applied to elastic waves. The rectangular region in Figure 0.1 has corners which can create instabilities in calculations. In Section 4, we discuss a theoretical procedure which trivially guarantees stability at the corners. This procedure suggests several simple and effective strategies involving modifications only at the corner point and its two adjacent discrete boundary points. In practice one is given a fixed difference scheme in the interior. In the process described in (b) and (c) above, the continuous radiating boundary condition is developed first and then discretized. When

there are only a small number of grid points per wave length, sometimes a more effective strategy is to fit the discrete radiating boundary conditions directly to the difference scheme itself. In Section 5, we analyze this alternative in a model problem where the analytic perfectly radiating boundary condition is local and all reflected errors are due to discretization. Finally, in Section 6, we use all of the methods and strategies discussed above and report on comparison calculations using frozen and variable coefficient radiating boundary conditions on a region as in Figure 0.1 with a variety of variable velocity media. In Appendix A, we present a standard derivation of the variable coefficient theoretical formulas using the calculus of pseudo-differential operators. In Appendix B, we discretize these analytic formulae to provide a catalogue of discrete radiating boundary conditions which we used in Section 6 and which we have found useful in practice.

Further work with various coauthors is in progress to develop radiating boundary conditions for the migration equations of exploration seismology and the unsteady small disturbance equation of transonic flow. We also speculate that our methods may be useful in treating the “vertical layer” in the global circulation models of meteorology where the alternative approach currently in practice of introducing a “viscous layer” can use as much as 25% of the computational grid points.

We apologize in advance to both our “theoretical” and “applied” readers for repeating a few already familiar details which we found necessary to reach both audiences.

1. Theoretical Analysis of Radiation Boundary Conditions for a Model Problem

Our objective here is to examine the simplest model of the wave behavior typified by the problems described in connection with Figure 0.1 and to provide for this model a rigorous analysis indicating that the approach developed by the authors in [4] is necessarily successful. In the course of this analysis, we shall also recall some of the theoretical procedures used in constructing these radiation boundary conditions (see [4]). Numerical evidence for the utility of the approach in this model problem has already been reported in [4].

The model problem has a solution, $u(x, y, t)$, which we must approximate, satisfying

$$\begin{aligned} \square u &= \left(\frac{\partial^2}{\partial t^2} - \left(\frac{\partial^2}{\partial x^2} + \frac{\partial^2}{\partial y^2} \right) \right) u = 0, & x \geq 0, t \geq 0, \\ (1.1) \quad u(0, y, t) &= g(y, t), \\ u &\text{ vanishes for } t \leq 0. \end{aligned}$$

Here $g(y, t)$ is an arbitrary square-integrable source function vanishing for

$t \geq 0$. Suppose δ , an acceptable error, and $a_0 > 0$ are given in advance. Following [4], our objective is to find a boundary condition, \mathcal{B} , on the wall $x = a$ with $a \geq a_0$ but as close to a_0 as possible so that if v is the solution of

$$(1.2) \quad \begin{aligned} \square v &= 0, \\ v(0, y, t) &= g(y, t), \\ \mathcal{B}v|_{x=a} &= 0, \\ v &\text{ vanishes for } t \leq 0, \end{aligned}$$

then

$$(1.3) \quad \left(\int_0^T \int_{-\infty}^{\infty} \int_0^{a_0} |u - v|^2 dx dy dt \right)^{1/2} \leq \delta$$

for times T so large that the travel time of the waves might produce M reflections from the artificial boundary at $x = a$, where M is a given positive integer. Additionally, practical considerations dictate that the boundary condition \mathcal{B} should be

$$(1.4) \quad \begin{aligned} &\text{(i) local,} \\ &\text{(ii) a well-posed boundary condition for } \square. \end{aligned}$$

Obviously, in order that (1.3) can be satisfied, the boundary conditions \mathcal{B} should also “minimize the amplitude of reflected waves”.

We consider the sequence of local boundary conditions \mathcal{B}_N on the finite wall $x = a$ given recursively by

$$(1.5) \quad \begin{aligned} \mathcal{B}_1 v \Big|_{x=a} &= \frac{\partial v}{\partial t} + \frac{\partial v}{\partial x} \Big|_{x=a} = 0, \\ \mathcal{B}_2 v \Big|_{x=a} &= \left(\frac{\partial^2 v}{\partial t^2} + \frac{\partial^2 v}{\partial t \partial x} - \frac{1}{2} \frac{\partial^2 v}{\partial y^2} \right) \Big|_{x=a} = 0, \\ \mathcal{B}_{N+1} v \Big|_{x=a} &= \left(\frac{\partial}{\partial t} \mathcal{B}_N(v) - \frac{1}{4} \frac{\partial^2}{\partial y^2} \mathcal{B}_{N-1}(v) \right) \Big|_{x=a} = 0. \end{aligned}$$

As we shall see below, the \mathcal{B}_N are associated with a continued fraction expansion of the symbol of a non-local operator and we call the \mathcal{B}_N the Padé boundary conditions. The boundary operators \mathcal{B}_1 , \mathcal{B}_2 , and \mathcal{B}_3 were already introduced in [4]. Let v_N denote the solution of (1.2) with the boundary condition $\mathcal{B} \equiv \mathcal{B}_N$. The following theorem holds:

THEOREM 1. (a) *Every \mathcal{B}_N is a local strongly well-posed boundary condition for the wave equation.*

(b) Given δ , an acceptable error, $a_0 > 0$, an integer $M > 0$, and an arbitrary source function $g(y, t)$ satisfying

$$\left(\int_0^\infty \int_{-\infty}^\infty |g(y, t)|^2 dy dt \right)^{1/2} = F < \infty,$$

there is an $a \geq a_0$ and an N so that if v_N solves the boundary value problem in (1.2) with $\mathcal{B} = \mathcal{B}_N$, then

$$\left(\int_0^T \int_0^{a_0} \int_{-\infty}^\infty |u - v_N|^2 dy dx dt \right)^{1/2} < \delta$$

for any time T with $0 \leq T \leq 2aM$.

Remark 1. It is not a trivial matter to construct well posed boundary conditions since the authors have observed in [4] that using Taylor approximations rather than continued fraction expansions can result in *strongly unstable* boundary conditions which are useless for practical calculations.

Remark 2. The distance a and the number N are important parameters in a practical calculation. The proof given below crudely indicates the dependence of a and N on the frequency distribution of g . Let

$$\hat{g}(\xi, \omega) = \frac{1}{(2\pi)^2} \iint \exp\{-i\xi t - i\omega y\} g(y, t) dy dt$$

be the Fourier transform of g and, for any $\epsilon_0 > 0$, define three regions by

$$G_1 = \left\{ (\xi, \omega) \mid 1 - \epsilon_0 \leq \frac{\omega^2}{\xi^2} \leq 1 + \epsilon_0 \text{ or } |\xi|^2 + |\omega|^2 < \epsilon_0 \right\}$$

(the glancing region),

$$G_2 = \left\{ (\xi, \omega) \mid \frac{\omega^2}{\xi^2} < 1 - \epsilon_0, |\xi|^2 + |\omega|^2 > \epsilon_0 \right\}$$

(the region of hard reflection),

$$G_3 = \left\{ (\xi, \omega) \mid \frac{\omega^2}{\xi^2} > 1 + \epsilon_0, |\xi|^2 + |\omega|^2 > \epsilon_0 \right\}$$

(the evanescent region),

and consider

$$F_j = \left(\iint_{G_j} |\hat{g}|^2 d\xi d\omega \right)^{1/2} \quad \text{for } j = 1, 2, 3.$$

The amplitude of g in the glancing region G_1 determines the size of ϵ_0 by the

condition $\sqrt{2a_0}MF_1 < \frac{1}{3}\delta$. Once ε_0 is given, the size of a is controlled by the strength of the “evanescent boundary layer” in the region G_3 and satisfies an inequality of the form $\exp\{(a_0 - 2a)b(\varepsilon_0)\}CF_3\sqrt{a_0} \leq \frac{1}{3}\delta$, where $b(\varepsilon_0) > 0$ is determined by ε_0 . Finally, the requirement

$$\max_{0 \leq x \leq 1 - \varepsilon_0} |(1 - x^2)^{1/2} - P_N(x)| F_2 \leq \frac{\delta}{3C},$$

where $P_N(x)$ is the N -th continued function expansion of $(1 - x^2)^{1/2}$ (and C is a universal constant), determines the size of N . For the numerical calculations reported in [4], the choice of $N = 2$ typically resulted in errors within δ given by 1–1.5% of the amplitude of the exact solution.

Below we shall often use the correspondence $i\xi \leftrightarrow \partial/\partial t$, $i\omega \leftrightarrow \partial/\partial y$ and, for $s = i\xi + \eta$ with $\eta \geq 0$, we let $\hat{g}(s, \omega) \equiv \widehat{\exp\{-\eta t\}g}$ denote the Laplace transform. Also, we choose the square root branch well-defined for $-\pi < \arg z < \pi$ with the implicit understanding that $\sqrt{x} = \pm i\sqrt{|x|}$ when $x < 0$ is a limit of the form $x = \lim_{y \rightarrow 0} (x + iy)$ with $y > 0$ or $y < 0$, respectively. Without loss of generality, we can assume below that g is sufficiently smooth and then pass to the limit.

A recipe for constructing the \mathcal{B}_N . Using the Laplace transform, we compute that the solution u to (1.1) is given for any $\eta > 0$ by

$$(1.6) \quad \exp\{-\eta t\}u(x, y, t) = \iint \exp\{-x(s^2 + \omega^2)^{1/2} + i\xi t + i\omega y\} \hat{g}(s, \omega) d\xi d\omega,$$

so that letting $\eta \rightarrow 0$ we obtain

$$(1.7) \quad u(x, y, t) = \iint \exp\{i\xi(-x(1 - \omega^2/\xi^2)^{1/2} + t) + i\omega y\} \hat{g}(\xi, \omega) d\xi d\omega.$$

If we introduce the operator which is non-local in space and time, defined by

$$\mathcal{R}u|_{x=a} = \iint \exp\{i\xi t + i\omega y\} i\xi(1 - \omega^2/\xi^2)^{1/2} \hat{u}(a, \xi, \omega) d\xi d\omega,$$

we compute trivially that the solution u satisfies the non-local theoretical radiation boundary condition on $x = a$ given by

$$(1.8) \quad \left(\frac{\partial u}{\partial x} + \mathcal{R} \right) \Big|_{x=a} = 0.$$

To develop the boundary conditions \mathcal{B}_N to be used as the local well-posed radiation boundary conditions on $x = a$, we use the finite continued fraction

expansions for $(1-x^2)^{1/2}$ given recursively by

$$\begin{aligned} P_1 &= 1, \\ P_2 &= 1 - \frac{x^2}{2}, \\ &\vdots \\ P_{N+1} &= 1 - \frac{x^2}{1 + P_N} \equiv 1 + \frac{T_{N+1}}{S_{N+1}}, \\ &\vdots \end{aligned}$$

where T_{N+1} and S_{N+1} are even polynomials in x . These finite continued fractions possess the following elementary properties (easily established by induction): Given $\varepsilon_0 > 0$, there exists $a(\varepsilon_0) > 0$ such that

$$\begin{aligned} (1.9) \quad & \text{(i) for } x^2 \leq 1 - \varepsilon_0, \quad 0 < a(\varepsilon_0) < P_N(x) \leq 1, \quad P_N(1) > 0, \\ & \text{(ii) for } x^2 \leq 1 - \varepsilon_0, \quad \lim_{N \rightarrow \infty} \max_{x^2 \leq 1 - \varepsilon_0} |(1-x^2)^{1/2} - P_N(x)| = 0, \\ & \text{(iii) } (1-x^2)^{1/2} - P_N(x) = O(x^{2N}). \end{aligned}$$

For the polynomials T_{N+1} and S_{N+1} , it is a simple matter to derive the recursion relations

$$\begin{aligned} T_{N+1} &= 2T_N - x^2 T_{N-1}, \quad T_1 = 0, \quad T_2 = -\frac{1}{2}x^2, \\ S_{N+1} &= 2S_N - x^2 S_{N-1}, \quad S_1 = 1, \quad S_2 = 1, \end{aligned}$$

from which it follows by induction that

$$\begin{aligned} (1.10) \quad & \text{for } N \text{ odd: } \deg T_N(x^2) = N-1, \quad \deg S_N(x^2) = N-1, \\ & \text{for } N \text{ even: } \deg T_N(x^2) = N, \quad \deg S_N(x^2) = N-2, \\ & \text{for } N \text{ odd: } S_N(x^2) = (-1)^{(N-1)/2} x^{N-1} + O(x^{N-3}), \\ & \text{for } N \text{ even: } T_N(x^2) = (-1)^{N/2} x^N + O(x^{N-2}). \end{aligned}$$

To derive the \mathcal{B}_N we use the Fourier transform and rewrite the boundary condition in (1.8) as

$$0 = \frac{\partial \hat{u}}{\partial x} + i\xi \left(1 - \frac{\omega^2}{\xi^2}\right)^{1/2} \hat{u} \Big|_{x=a} = \frac{\partial \hat{u}}{\partial x} + i\xi P_N\left(\frac{\omega}{\xi}\right) \hat{u} \Big|_{x=a} + i\xi O\left(\left|\frac{\omega}{\xi}\right|^{2N}\right) \hat{u} \Big|_{x=a}$$

We clear the denominator to obtain the approximation

$$S_N\left(\frac{i\omega}{i\xi}\right)\frac{\partial\hat{u}}{\partial x} + i\xi\left(S_N\left(\frac{i\omega}{i\xi}\right) + T_N\left(\frac{i\omega}{i\xi}\right)\right)\hat{u}\Big|_{x=a} = 0$$

and observe from (1.10) that $\deg S_N(i\omega/i\xi) \leq N-1$ and $\deg T_N(i\omega/i\xi) \leq N$; thus

$$(1.11) \quad (i\xi)^{N-1}S_N\left(\frac{i\omega}{i\xi}\right)\frac{\partial}{\partial x} + (i\xi)^N S_N\left(\frac{i\omega}{i\xi}\right) + (i\xi)^N T_N\left(\frac{i\omega}{i\xi}\right) = \mathcal{B}_N\left(i\xi, i\omega, \frac{\partial}{\partial x}\right)$$

is a polynomial of degree at most N in (ξ, ω) . If we define $\mathcal{B}_N(\partial/\partial t, \partial/\partial y, \partial/\partial x)$ using the correspondence $i\xi \rightarrow \partial/\partial t$, $i\omega \leftrightarrow \partial/\partial y$, then $\mathcal{B}_N(\partial/\partial t, \partial/\partial y, \partial/\partial x)$ is the local Padé boundary condition on $x = a$ for which we shall verify Theorem 1. It is easily checked using the identities above (1.10) that

$$\mathcal{B}_{N+1}(i\xi, i\omega, \partial/\partial x) = i\xi \mathcal{B}_N(i\xi, i\omega, \partial/\partial x) + \frac{1}{4}\omega^2 \mathcal{B}_{N-1}(i\xi, i\omega, \partial/\partial x);$$

therefore the \mathcal{B}_N are computed in the fashion described in (1.5).

The error estimate—the proof of part (b). We first prove part (b) assuming part (a) and then we verify part (a). Associated with the boundary condition \mathcal{B} and the exponential with $\Re s \geq 0$ given by

$$\exp\{-(s^2 + \omega^2)^{1/2}x + st + i\omega y\}$$

is the *reflection coefficient* $R_N(s, i\omega)$ defined by

$$(1.12) \quad R_N(s, i\omega) = \frac{-(s^2 + \omega^2)^{1/2} + sP_N(i\omega/s)}{(s^2 + \omega^2)^{1/2} + sP_N(i\omega/s)}.$$

In the course of proving part (a), we shall verify that $R_N(s, i\omega)$ is a holomorphic function in $\Re s > 0$ satisfying

$$(1.13) \quad |R_N(s, i\omega)| \leq 1, \quad \Re s \geq 0.$$

Using the Fourier–Laplace transform and the holomorphic character of the reflection coefficient, one verifies that the solution v_N of (1.2) with $\mathcal{B} = \mathcal{B}_N$ is given by

$$(1.14) \quad v_N = u_N + \sum_{j=1}^{\infty} v_N^j,$$

where

$$(1.15) \quad \begin{aligned} v_N^j = & \iint \exp\{(x - 2ja)i\xi(1 - \omega^2/\xi^2)^{1/2} + i\xi t + i\omega y\}(-1)^j R(i\xi, i\omega) \hat{g} \, d\xi \, du \\ & + \iint \exp\{-(x + 2ja)i\xi(1 - \omega^2/\xi^2)^{1/2} + i\xi t + i\omega y\}(-1)^{j+1} R_N^j(i\xi, i\omega) \hat{g} \, d\xi \, d\omega. \end{aligned}$$

Furthermore, it follows in standard fashion from (1.13) and the Paley–Wiener

theorem that, given T with $T \leq 2aM$, $v_N^j(x, y, t) \equiv 0$ for $t \leq T$ and $j > M$. To establish the conclusion in part (b), by Plancherel's theorem, we need only verify that

$$(1.16) \quad \sum_{j=1}^M \left(\int_{-\infty}^{\infty} \int_{-\infty}^{\infty} \int_0^{a_0} |\hat{v}_N^j|^2 dx d\omega d\xi \right)^{1/2} < \delta.$$

Recall the definition of G_i and F_i , $i = 1, 2, 3$, given above. By (1.13), we estimate the glancing contributions by

$$(1.17) \quad \sum_{j=1}^M \left(\int_{G_1} \int_0^{a_0} |\hat{v}_N^j|^2 dx d\xi d\omega \right)^{1/2} \leq (2a_0)^{1/2} M F_1 < \frac{1}{3} \delta$$

provided that ε_0 is chosen so small that

$$\int_{G_1} |\hat{g}(\xi, \omega)|^2 \leq \frac{\delta}{3(2a_0)^{1/2} M}.$$

Next, we estimate the contributions from the region G_2 corresponding to hard reflections—here the absorbing properties of the boundary condition \mathcal{B}_N are crucial. By properties (i) and (ii) in (1.9), given δ' and ε_0 , there exists N such that

$$(1.18) \quad \min_{x^2 \leq 1 - \varepsilon_0} |(1 - x^2)^{1/2} + P_N(x)| \geq \sqrt{2\varepsilon_0} + a(\varepsilon_0) > 0,$$

$$\max_{x^2 \leq 1 - \varepsilon_0} |(1 - x^2)^{1/2} - P_N(x)| < \delta'(\sqrt{2\varepsilon_0} + a(\varepsilon_0))^{-1}.$$

Using the definition in (1.12) and the properties in (1.18), we verify that

$$\max_{(\xi, \omega) \in G_2} |R_N(i\xi, i\omega)| < \delta'.$$

Thus (with $\delta' < 1$)

$$(1.19) \quad \sum_{j=1}^M \left(\int_{G_2} \int_0^{a_0} |\hat{v}_N^j|^2 dx d\omega d\xi \right)^{1/2} \leq \sqrt{2a_0} F_2 \delta' \left(\frac{1 - (\delta')^M}{1 - \delta'} \right) \leq \frac{1}{3} \delta,$$

by choosing δ' appropriately. Finally, we estimate the evanescent boundary layer from the region G_3 ; here only the stability properties of the boundary conditions as expressed in (1.13) enter in the estimates. On the region G_3 , $\omega^2/\xi^2 \geq 1 + \varepsilon_0$ and $(|\xi|^2 + |\omega|^2)^{1/2} \geq \sqrt{\varepsilon_0}$; thus

$$\max_{(\xi, \omega) \in G_3} (\omega^2 - \xi^2)^{1/2} \geq b(\varepsilon_0) > 0.$$

From this fact follows the simple estimate

$$\max_{\substack{(\xi, \omega) \in G_3 \\ 0 \leq x \leq a_0}} (|\exp\{(x - 2ja)(\omega^2 - \xi^2)^{1/2}\}|, |\exp\{-(x + 2ja)(\omega^2 - \xi^2)^{1/2}\}|) \\ \leq \exp\{(a_0 - 2ja)b(\varepsilon_0)\}.$$

Thus, given δ ,

$$(1.20) \quad \sum_{i=1}^M \left(\int_{G_2} \int_0^{a_0} |\hat{v}_N^i|^2 dx d\xi d\omega \right)^{1/2} \leq (2a_0)^{1/2} \exp \{ -(2a - a_0)b(\epsilon_0) \} \left(\frac{1 - \exp \{-2aMb(\delta)\}}{1 - \exp \{-2ab(\delta)\}} \right) F_3 \leq \frac{1}{3}\delta,$$

provided that a is chosen sufficiently large. Adding (1.17), (1.19), and (1.20), we complete the proof of part (b).

Stability of the Padé boundary conditions—the proof of part (a). We begin by recalling the general algebraic normal mode analysis for checking well-posedness for mixed boundary value problems specialized here to the variable coefficient wave equation (see Kreiss [6]).

DEFINITION. A boundary condition \mathcal{B}_N on the wall $x=0$ together with the wave equation acting on functions defined in $x \leq 0, t \geq 0$ is *strongly well-posed* provided that there are no solutions of the form

$$w(s, \omega) = \exp \{s^2 + \omega^2\}^{1/2} x + st + i\omega y\}$$

with $\Re s \geq 0$ satisfying

$$(1.21) \quad \begin{aligned} \square w(s, \omega) &= 0 \quad \text{in } x < 0, \\ \mathcal{B}_N w(s, \omega)|_{x=0} &= 0. \end{aligned}$$

Furthermore, for $|s|^2 + |\omega|^2 = 1$ and $\Re s \geq 0$, $\mathcal{B}_N w(s, \omega)$ should satisfy

$$(1.22) \quad |\mathcal{B}_N(w(s, \omega))| \geq c_0 > 0.$$

We also recall the definition of well-posedness for initial value problems with $x > 0$ as the evolution direction.

DEFINITION. The scalar initial value problem

$$\begin{aligned} \left(A_1 \left(\frac{\partial}{\partial t}, \frac{\partial}{\partial y} \right) \frac{\partial}{\partial x} + A_2 \left(\frac{\partial}{\partial t}, \frac{\partial}{\partial y} \right) \right) u &= 0, & x > 0, \\ u(x, 0) &= u_0(x), \end{aligned}$$

with $A_1(\xi, \omega), A_2(\xi, \omega)$ homogeneous polynomials of degree $N-1, N$, respectively, is (weakly) well posed as an evolution operator in x in the direction

$x > 0$ provided that whenever K satisfies

$$(1.23) \quad A_1(i\xi, i\omega)K + A_2(i\xi, i\omega) = 0$$

with $|\xi|^2 + |\omega|^2 > 0$, then $\Re_e K \leq 0$.

With these preliminary facts, we begin the proof of (a) by claiming that

$$(1.24) \quad \mathcal{B}_N \text{ is a (weakly) well-posed evolution operator for } x > 0.$$

When $\xi \neq 0$, (1.11) and (1.23) imply that

$$K + i\xi P_N \left(\frac{i\omega}{i\xi} \right) = 0$$

and, because P_N has real coefficients, that $\Re_e K = 0$. On the other hand, when $\xi = 0$, it follows from (1.10) and (1.11) that

$$(1.25) \quad \begin{aligned} \text{for } N \text{ odd: } & (-1)^{(N-1)/2} (i\omega)^{N-1} K = 0, \\ \text{for } N \text{ even: } & (-1)^{N/2} (i\omega)^N = 0. \end{aligned}$$

Thus, in the first case, $K = 0$ while, in the second, no root K exists. This verifies the claim in (1.24). As our next step we derive the following general fact:

PROPOSITION 1.1. *Assume $\mathcal{B}_N(i\xi, i\omega, K)$ is homogeneous of degree N and has the form*

$$\frac{\partial^N}{\partial t^N} + P_N^1 \left(\frac{\partial}{\partial t}, \frac{\partial}{\partial y} \right) \frac{\partial}{\partial x} + P_N^2 \left(\frac{\partial}{\partial t}, \frac{\partial}{\partial y} \right) \frac{\partial}{\partial y},$$

where $P_N^1(i\xi, i\omega)$, $P_N^2(i\xi, i\omega)$ are homogeneous of degree $N-1$. Also assume that \mathcal{B}_N as an evolution operator in x with direction $x \geq 0$ is well-posed. Then, given ω, K with $\Re_e K > 0$, the number of roots $\tau_j(\omega, K)$ satisfying $\mathcal{B}_N(\tau_j, i\omega, K) = 0$ and $\Re_e \tau_j > 0$ is a constant independent of ω and K with $\Re_e K > 0$. In particular, when \mathcal{B}_N is given by the Padé boundary condition, this number of roots is zero independent of K and ω with $\Re_e K > 0$.

Proof: For fixed (ω, K) , $\mathcal{B}_N(\tau, i\omega, K)$ is a polynomial of degree N in τ with N roots which are continuous functions of the parameters $(i\omega, K)$. Thus, if the number of roots τ_j with $\Re_e \tau_j > 0$ is not constant, then there are ω_0 and K_0 with $\Re_e K_0 > 0$ and a purely imaginary root $\tau = i\xi_0$ satisfying $\mathcal{B}_N(i\xi_0, i\omega_0, K_0) = 0$ but this contradicts the fact that \mathcal{B}_N is a well-posed

evolution operator with direction $x > 0$. Applying the first part of this proposition to the Padé boundary conditions, we need only count the roots τ with $\Re \tau > 0$ when $i\omega \equiv 0$ but, according to (1.11), these satisfy

$$0 = (K + \tau)\tau^{N-1}$$

and since $\Re K > 0$, the proof of the last line of the proposition is complete.

The last sentence in the proposition already implies that the first condition of well-posedness from (1.21) is satisfied. Suppose

$$w(s, \omega) = \exp \{(s^2 + \omega^2)^{1/2}x + st + i\omega y\}$$

with $\Re s > 0$ satisfies $\square w(s, \omega) = 0$ and $\mathcal{B}_N|w(s, \omega)|_{x=0} = 0$. Setting $K = (s^2 + \omega^2)^{1/2}$, $\tau = s$; then (τ, K) satisfy $\mathcal{B}_N(\tau, i\omega, K) = 0$ with $\Re K > 0$ and $\Re \tau > 0$ and this contradicts the proposition. Therefore, to verify the condition in (1.22) by compactness and the previous statement, we need only verify that, for fixed $s = i\xi$ with $|\xi|^2 + |\omega|^2 = 1$,

$$(1.26) \quad \left| (i\xi)^N S_N\left(\frac{i\omega}{i\xi}\right) \left(1 - \frac{\omega^2}{\xi^2}\right)^{1/2} + (i\xi)^N \left(S_N\left(\frac{i\omega}{i\xi}\right) + T_N\left(\frac{i\omega}{i\xi}\right)\right) \right| \neq 0.$$

Once again there are two cases; for $\xi \neq 0$, the condition in (1.26) is equivalent to

$$\left| \left(1 - \frac{\omega^2}{\xi^2}\right)^{1/2} + P_N\left(\frac{i\omega}{i\xi}\right) \right| > 0.$$

For $\omega^2/\xi^2 \geq 1$, this term never vanishes because $(1 - \omega^2/\xi^2)^{1/2}$ is imaginary and vanishes at $\omega^2/\xi^2 = 1$ while P_N is real with $P_N(1) \neq 0$. For $\omega^2/\xi^2 < 1$, $(1 - \omega^2/\xi^2)^{1/2} > 0$ and from (i) of (1.9), $0 < P_N \leq 1$. When $\xi = 0$, the facts in (1.25) apply with K replaced by $\sqrt{\omega^2}$. This completes the proof of part (a) of Theorem 1.

Finally, we establish the estimate in (1.13) for the reflection coefficient R_N . Recall that

$$\begin{aligned} R_N(i\xi, i\omega) &= \frac{-(\omega^2 - \xi^2)^{1/2} + i\xi P_N(i\omega/i\xi)}{(\omega^2 - \xi^2)^{1/2} + i\xi P_N(i\omega/i\xi)} \\ &= \frac{-(1 - \omega^2/\xi^2)^{1/2} + P_N(i\omega/i\xi)}{(1 - \omega^2/\xi^2)^{1/2} + P_N(i\omega/i\xi)}, \quad \xi \neq 0. \end{aligned}$$

It follows from (1.21) that $R_N(s, i\omega)$ is holomorphic in s for $\Re s > 0$. For $s = i\xi$ and $\omega^2/\xi^2 \geq 1$, R_N has the form $R_N = (-ia + b)/(ia + b)$ which implies

that $|R_N(i\xi, i\omega)| = 1$ while, for $\omega^2/\xi^2 < 1$, R_N has the form $R_N(i\xi, i\omega) = (-a+b)/(a+b)$ with $a, b > 0$; thus $|R_N(i\xi, i\omega)| < 1$. By the third property of (1.10), $|\eta R_N(i\xi + \eta, i\omega)| < M$; thus the required estimate in (1.31) for $\Re s \geq 0$ follows from the maximum principle.

2. Frozen Coefficient and Variable Coefficient Radiation Boundary Conditions—An Analytic Comparison

Even simple seismic wave calculations require using variable velocities. In designing radiation boundary conditions at artificial computational boundaries, there are two distinct plans of attack.

- (i) *Frozen Coefficient Theory*: Freeze the coefficients of the differential equation at a point on the computational boundary and apply the constant coefficient radiation boundary conditions discussed in [4] and in Section 1 above.
- (ii) *Variable Coefficient Theory*: Develop radiation boundary conditions which account for the spatial variation of the velocity coefficients.

In [4], the authors sketched how a general variable coefficient theory of radiating boundary conditions can be developed using the theory of pseudo-differential operators. In this section we give an analytic comparison of the frozen coefficient versus variable velocity model which has exact solutions given by Airy functions.

The model problem which we study has general solutions u , satisfying the equations

$$(2.1) \quad \begin{aligned} (1+x) \frac{\partial^2 u}{\partial t^2} - \frac{\partial^2 u}{\partial x^2} - \frac{\partial^2 u}{\partial y^2} &= 0, & x > 0, t \geq 0, \\ u(0, y, t) &= g(y, t), \\ u \text{ vanishes for } t &\leq 0. \end{aligned}$$

Here g is a square integrable source vanishing for $t \leq 0$. Our objective is to design radiation boundary conditions on the wall $x = a$ with $a > 0$. By using the Fourier-Laplace transform, we compute that the exact solution u is given by

$$(2.2) \quad u(x, y, t) = \iint \exp \{i\xi t + i\omega y\} \frac{\text{Ai}((i\xi)^{2/3}(1+x-\omega^2/\xi^2))}{\text{Ai}((i\xi)^{2/3}(1-\omega^2/\xi^2))} \hat{g}(\xi, \omega) d\xi d\omega,$$

where $\text{Ai}(z)$ is the Airy function satisfying

$$\frac{d^2 \text{Ai}(z)}{dz^2} - z \text{Ai}(z) = 0.$$

It is well known (see [10]) that Ai has the uniform asymptotic expansion

$$(2.3) \quad \text{Ai}(z) \sim \frac{1}{2}\pi^{-1/2} z^{-1/4} e^{-i\varphi} \sum_{k=0}^{\infty} \frac{(-1)^k \Gamma(3k + \frac{1}{2})}{6^k k! \Gamma(k + \frac{1}{2})} z^{-3k/2}$$

valid for $-\pi < \arg z < \pi$, where $\varphi = \frac{2}{3}z^{3/2}$, and that this expansion when differentiated term by term is the asymptotic expansion for $\text{Ai}(z)$. For future reference, we define

$$(2.4) \quad \begin{aligned} z(x, \xi, \omega) &= (i\xi)^{2/3} \left(1 + x - \frac{\omega^2}{\xi^2} \right), \\ \varphi(x, \xi, \omega) &= \frac{2}{3}i\xi \left(1 + x - \frac{\omega^2}{\xi^2} \right)^{3/2}. \end{aligned}$$

In general it is not possible to write down an explicit theoretical radiation boundary condition for a variable velocity wave equation and this is the reason why an approximate theory (as developed in Appendix A) is needed. However, one of the reasons motivating the choice of the model equation in (2.1) is that, in this special case, it follows from the solution formula in (2.2) that u satisfies the *explicit theoretical radiation boundary* condition given by

$$\left(\frac{d}{dx} + \mathcal{R}_a \right) u \Big|_{x=a} = 0,$$

where

$$(2.5) \quad \mathcal{R}_a = \iint \exp \{ i\xi t + i\omega y \} (i\xi)^{2/3} \frac{\text{Ai}'((i\xi)^{2/3}(1 + a - \omega^2/\xi^2))}{\text{Ai}((i\xi)^{2/3}(1 - \omega^2/\xi^2))} \hat{u}(\xi, \omega, a) d\xi d\omega.$$

The frozen coefficient theory. To develop radiation boundary conditions on the wall $x = a$ by means of the frozen coefficient theory, we consider the constant coefficient operator

$$(1 + a) \frac{\partial^2}{\partial t^2} - \left(\frac{\partial^2}{\partial x^2} + \frac{\partial^2}{\partial y^2} \right).$$

By using the correspondence $i\xi \leftrightarrow \partial/\partial t$, $i\omega \leftrightarrow \partial/\partial y$, after taking a Fourier transform, we factor this operator into the form

$$(2.6) \quad \begin{aligned} \frac{\partial^2}{\partial x^2} + (1 + a)\xi^2 - \omega^2 &= \left(\frac{\partial}{\partial x} - i\xi(1 + a)^{1/2} \left(1 - \frac{\omega^2}{(1 + a)\xi^2} \right)^{1/2} \right) \\ &\quad \times \left(\frac{\partial}{\partial x} + i\xi(1 + a)^{1/2} \left(1 - \frac{\omega^2}{(1 + a)\xi^2} \right)^{1/2} \right). \end{aligned}$$

Thus, from (2.6) it follows that the (approximate) theoretical radiating boundary condition predicted by the frozen coefficient theory is given by

$$(2.7) \quad \left(\frac{\partial}{\partial x} + i\xi(1+a)^{1/2} \left(1 - \frac{\omega^2}{(1+a)\xi^2} \right)^{1/2} \right) \hat{u}(x, \xi, \omega) \Big|_{x=a} = 0.$$

Using the first and second expansions as in [4] or Section 1, we compute the 1-st and 2-nd approximate local radiating boundary conditions \mathcal{B}_1^F and \mathcal{B}_2^F , given by the frozen coefficient theory, as

$$(2.8) \quad \begin{aligned} \mathcal{B}_1^F v|_{x=a} &= \left(\frac{\partial}{\partial x} + (1+a)^{1/2} \frac{\partial}{\partial t} \right) v \Big|_{x=a} = 0, \\ \mathcal{B}_2^F v|_{x=a} &= \left(\frac{\partial^2}{\partial x \partial t} + (1+a)^{1/2} \frac{\partial^2}{\partial t^2} - \frac{1}{2} \frac{1}{(1+a)^{1/2}} \frac{\partial^2}{\partial y^2} \right) v \Big|_{x=a} = 0. \end{aligned}$$

The variable coefficient theory. As we have mentioned previously, for general operators it is not possible to calculate the theoretical boundary condition in (2.5) explicitly. However, by using the theory sketched in the appendix, one can in general write down an asymptotic approximation to this theoretical radiation boundary condition valid for $|\xi| \rightarrow \infty$. When applied to the case $\nu^2 = 1+x$ and the wall $x=a$, the second-order approximate theoretical radiating boundary condition is given by

$$\left(\frac{\partial}{\partial x} - (\lambda_-^+ + \lambda_-^0 + \lambda_-^{-1}) \right) \hat{u}(x, \xi, \omega) \Big|_{x=a} = 0.$$

Choosing $\nu^2 = 1+x$ in formula (A.10) of the appendix, the above condition becomes

$$(2.9) \quad \begin{aligned} & \left(\frac{\partial}{\partial x} + (1+a)^{1/2} i\xi \left(1 - \frac{\omega^2}{(1+a)\xi^2} \right)^{1/2} + \frac{1}{4} \frac{1}{(1+a) - \omega^2/\xi^2} \right. \\ & \quad \left. - \frac{5}{32} \frac{1}{i\xi} \left(1 + a - \frac{\omega^2}{\xi^2} \right)^{-5/2} \right) \hat{u} \Big|_{x=a} = 0, \end{aligned}$$

so that, by repeating the procedure in [4] or Section 1, we obtain the variable coefficient local radiating boundary conditions $\mathcal{B}_1^V, \mathcal{B}_2^V$, given by

$$(2.10) \quad \begin{aligned} \mathcal{B}_1^V(v) &= \left(\frac{\partial}{\partial x} + (1+a)^{1/2} \frac{\partial}{\partial t} + \frac{1}{4} \frac{1}{1+a} \right) v \Big|_{x=a} = 0, \\ \mathcal{B}_2^V(v) &= \left(\frac{\partial^2}{\partial x \partial t} + (1+a)^{1/2} \frac{\partial^2}{\partial t^2} - \frac{1}{(1+a)^{1/2}} \frac{\partial^2}{\partial y^2} \right. \\ & \quad \left. + \frac{1}{4} \frac{1}{1+a} \frac{\partial}{\partial t} - \frac{5}{32} (1+a)^{-5/2} \right) v \Big|_{x=a} = 0. \end{aligned}$$

We remark that the highest-order terms of $\mathcal{B}_1^V, \mathcal{B}_2^V$ agree with \mathcal{B}_1^F and \mathcal{B}_2^F , however the variable coefficient theory produces lower-order corrections in a systematic fashion to the constant coefficient theory.

Comparison of the methods. As discussed previously, the objective of our approach is to design a well-posed local boundary condition \mathcal{B} on the wall $x = a$ so that if v satisfies

$$(2.11) \quad \begin{aligned} \left((1+x) \frac{\partial^2}{\partial t^2} - \left(\frac{\partial^2}{\partial x^2} + \frac{\partial^2}{\partial y^2} \right) \right) v &= 0, & 0 < x < a, \\ v|_{x=0} &= g, \\ \mathcal{B}v|_{x=a} &= 0, \end{aligned}$$

then $|v - u| \leq \delta$ for $0 \leq t \leq T$, where u satisfies the equation (2.1) and δ is an acceptable error. Here, for simplicity in exposition, we shall assume that only a single wave gets reflected from the wall $x = a$ by the time T and that this wave has not reached $x = 0$. Because well-posedness of a mixed-boundary value problem is determined by checking the frozen coefficient case with lower-order terms, it follows that $\mathcal{B}_1^F, \mathcal{B}_2^F$, and $\mathcal{B}_1^V, \mathcal{B}_2^V$ are all well-posed boundary conditions. Under these circumstances, the solution v to (2.11) is given by $v = u + v^1$, where

$$(2.12) \quad v^1 = - \iint \exp \{ i\xi t + i\omega y \} \frac{\text{Ai}((-i\xi)^{2/3}(1+x-\omega^2/\xi^2))}{\text{Ai}((-i\xi)^{2/3}(1+a-\omega^2/\xi^2))} R_{\mathcal{B}}(\xi, \omega, a) \hat{u}(\xi, \omega, a) d\xi d\omega.$$

Here, analogous to Section 1, $R_{\mathcal{B}}$ is the reflection coefficient associated with the boundary condition \mathcal{B} on the wall $x = a$. Given a local boundary condition $\mathcal{B}(a, \partial/\partial t, \partial/\partial y, \partial/\partial x)$, this reflection coefficient is given by

$$(2.13) \quad \begin{aligned} R_{\mathcal{B}}(\xi, \omega, a) &\equiv \frac{\text{Ai}\left((-i\xi)^{2/3}\left(1+a-\frac{\omega^2}{\xi^2}\right)\right)}{\text{Ai}\left((i\xi)^{2/3}\left(1+a-\frac{\omega^2}{\xi^2}\right)\right)} \\ &\times \frac{\mathcal{B}\left(i\xi, i\omega, \frac{\partial}{\partial x}\right) \text{Ai}\left((i\xi)^{2/3}\left(1+x-\frac{\omega^2}{\xi^2}\right)\right)}{\mathcal{B}\left(a, i\xi, i\omega, \frac{\partial}{\partial x}\right) \text{Ai}\left((-i\xi)^{2/3}\left(1+x-\frac{\omega^2}{\xi^2}\right)\right)} \Big|_{x=a}. \end{aligned}$$

We remark that $R_{\mathcal{B}}$ is the only factor in the representation for the error, $v^1 \equiv u - v$, which depends upon the local boundary condition \mathcal{B} ; thus we

compare the magnitude of $R_{\mathfrak{B}}$ for the choices of \mathfrak{B} given by the frozen and variable coefficient theories in (2.8) and (2.10).

We define $D(\xi, \omega, a)$ by

$$(2.14) \quad D(\xi, \omega, a) = \frac{\text{Ai}'(z(\xi, \omega, a))}{\text{Ai}(z(\xi, \omega, a))}.$$

It follows from the formula (2.13) that the reflection coefficients for the frozen and variable coefficient theories are given by

$$(2.15) \quad \begin{aligned} R_{\mathfrak{B}_1^r}(\xi, \omega, a) &= \frac{(i\xi)^{2/3}D(\xi, \omega, a) + (1+a)^{1/2}i\xi}{(-i\xi)^{2/3}D(-\xi, \omega, a) + (1+a)^{1/2}i\xi}, \\ R_{\mathfrak{B}_2^r}(\xi, \omega, a) &= \frac{(i\xi)^{5/3}D(\xi, \omega, a) + (1+a)^{1/2}(i\xi)^2 - \frac{1}{2}(1+a)^{-1/2}(i\omega)^2}{(-i\xi)^{2/3}i\xi D(-\xi, \omega, a) + (1+a)^{1/2}(i\xi)^2 - \frac{1}{2}(1+a)^{-1/2}(i\omega)^2}, \\ R_{\mathfrak{B}_1^v}(\xi, \omega, a) &= \frac{(i\xi)^{2/3}D(\xi, \omega, a) + (1+a)^{1/2}i\xi + \frac{1}{4}(1+a)^{-1}}{(-i\xi)^{2/3}D(-\xi, \omega, a) + (1+a)^{1/2}i\xi + \frac{1}{4}(1+a)^{-1}}, \\ R_{\mathfrak{B}_2^v}(\xi, \omega, a) &= \frac{(i\xi)^{5/3}D(\xi, \omega, a) + (1+a)^{1/2}(i\xi)^2 - \frac{1}{2}(1+a)^{-1/2}(i\omega)^2 + \frac{1}{4}i\xi(1+a)^{-1} + \frac{5}{32}(1+a)^{-5/2}}{(i\xi)(-i\xi)^{2/3}D(-\xi, \omega, a) + (1+a)^{1/2}(i\xi)^2 - \frac{1}{2}(1+a)^{-1/2}(i\omega)^2 + \frac{1}{4}i\xi(1+a)^{-1} - \frac{5}{32}(1+a)^{-5/2}}. \end{aligned}$$

Asymptotic comparison. It follows from the asymptotic expansion (2.3) that, as $|z(\xi, \omega, a)| \rightarrow \infty$,

$$(2.16) \quad D(\xi, \omega, a) \sim -z^{1/2} - \frac{1}{4}z^{-1} + \frac{1}{8}z^{-5/2} + O(|z|^{-4}),$$

where we recall that

$$z(\xi, \omega, a) = (i\xi)^{2/3}(1+a) \left(1 - \frac{\omega^2}{(1+a)\xi^2} \right).$$

Given a frequency pair (ξ_0, ω_0) , we choose a so that if α is defined by

$$\alpha = \frac{\omega_0^2}{(1+a)\xi_0^2},$$

then a is large enough so that $\alpha < 1$ —for any frequency (ξ_0, ω_0) which is not associated with the evanescent boundary layer at $x = 0$ (thus $\omega_0^2/\xi_0^2 \leq 1$) this condition is satisfied for any $a > 0$.

From (2.16) we derive that, as $\lambda \rightarrow \infty$,

$$(2.17) \quad \begin{aligned} (i\lambda\xi_0)^{2/3} D(\lambda\xi_0, \lambda\omega_0, a) &\sim -(i\lambda\xi_0)(1+a)^{1/2}(1-\alpha)^{1/2} \\ &\quad -\frac{1}{4}(1+a)^{-1}(1-\alpha)^{-1} + \frac{1}{8}(i\lambda\xi_0)^{-1}(1+a)^{-5/2} \\ &\quad + O(|\lambda|^{-2}(1+a)^{-4}(1-\alpha)^{-4}). \end{aligned}$$

We define R_1 and R_2 by

$$R_1 \equiv \frac{1-(1-\alpha)^{1/2}}{1+(1-\alpha)^{1/2}} \quad \text{and} \quad R_2 \equiv \frac{(1-\frac{1}{2}\alpha)-(1-\alpha)^{1/2}}{(1-\frac{1}{2}\alpha)+(1-\alpha)^{1/2}},$$

and comment that R_1 and R_2 are the reflection coefficients for the first and second approximations from Section 1 applied to the constant coefficient operator $(1+a) \partial^2/\partial t^2 - \partial^2/\partial x^2 - \partial^2/\partial y^2$. We also define $C_1^F(\alpha)$, $C_2^F(\alpha)$, $C_1^V(\alpha)$, $C_2^V(\alpha)$ by

$$\begin{aligned} C_1^F(\alpha) &= \frac{(1-\alpha)^{-1}(1-\alpha)^{1/2}}{(1+(1-\alpha)^{1/2})^2}, \\ C_2^F(\alpha) &= \frac{(1-\alpha)^{-1}(1-\alpha)^{1/2}}{((1-\frac{1}{2}\alpha)+(1-\alpha)^{1/2})^2}, \\ C_1^V(\alpha) &= \frac{((1-\alpha)^{-1}-1)(1-\alpha)^{1/2}}{(1+(1-\alpha)^{1/2})^2}, \\ C_2^V(\alpha) &= \frac{((1-\alpha)^{-1}-1)(1-\alpha)^{1/2}}{(1+(1-\alpha)^{1/2})^2}. \end{aligned}$$

It is easily verified that these functions satisfy

$$(2.18) \quad \begin{aligned} R_1(0) &= R_2(0) = 0, \\ R_1'(0) &= 1 \quad \text{and} \quad R_2'(0) = 0, \\ 0 &< R_1(\alpha) < R_2(\alpha) \quad \text{for} \quad 0 < \alpha < 1, \end{aligned}$$

and

$$(2.19) \quad \begin{aligned} C_1^F(0) &= C_2^F(0) = \frac{1}{2}, \\ C_1^V(0) &= C_2^V(0) = 0, \\ 0 &< C_1^V(\alpha) < C_2^V(\alpha) < C_1^F(\alpha) < C_2^F(\alpha) \quad \text{for} \quad 0 < \alpha < 1. \end{aligned}$$

By plugging (2.17) into (2.15), we see that, as $\lambda \rightarrow \infty$, there exists $C(\varepsilon_0)$ such

that, for $0 \leq \alpha \leq 1 - \varepsilon_0$,

$$\begin{aligned}
 R_{\mathfrak{A}_1^F}(\lambda \xi_0, \lambda \omega_0, a) &\sim R_1(\alpha) + i \frac{(1+a)^{-3/2}}{2\xi_0 \lambda} C_1^F(\alpha) + O(C(\varepsilon_0)|\lambda|^{-2}), \\
 R_{\mathfrak{A}_1^V}(\lambda \xi_0, \lambda \omega_0, a) &\sim R_1(\alpha) + i \frac{(1+a)^{-3/2}}{2\xi_0 \lambda} C_1^V(\alpha) + O(C(\varepsilon_0)|\lambda|^{-2}), \\
 R_{\mathfrak{A}_2^F}(\lambda \xi_0, \lambda \omega_0, a) &\sim R_2(\alpha) + i \frac{(1+a)^{-3/2}}{2\xi_0 \lambda} C_2^F(\alpha) + O(C(\varepsilon_0)|\lambda|^{-2}), \\
 R_{\mathfrak{A}_2^V}(\lambda \xi_0, \lambda \omega_0, a) &\sim R_2(\alpha) + i \frac{(1+a)^{-3/2}}{2\xi_0 \lambda} C_2^V(\alpha) + O(C(\varepsilon_0)|\lambda|^{-2}).
 \end{aligned}
 \tag{2.20}$$

From (2.18), (2.19), and (2.20) we deduce the following facts:

PROPOSITION 2.1 *Set $\alpha = \omega_0^2/\xi_0^2(1+a)$. If $0 < \alpha < 1$, then within asymptotic errors of $O(C(\varepsilon_0)|\lambda|^{-2})$, as $\lambda \rightarrow \infty$,*

$$(2.21) \quad |R_{\mathfrak{A}_2^V}(\lambda \xi_0, \lambda \omega_0, a)| < |R_{\mathfrak{A}_2^F}(\lambda \xi_0, \lambda \omega_0, a)| < |R_{\mathfrak{A}_1^V}| < |R_{\mathfrak{A}_1^F}|.$$

At normal incidence (when $\alpha = 0$) within asymptotic errors of $O(C(\varepsilon_0)|\lambda|^{-2})$, as $\lambda \rightarrow \infty$,

$$(2.22) \quad 0 = |R_{\mathfrak{A}_2^V}(\lambda \xi_0, \lambda \omega_0, a)| = |R_{\mathfrak{A}_1^V}(\lambda \xi_0, \lambda \omega_0, a)| < |R_{\mathfrak{A}_1^F}| < |R_{\mathfrak{A}_2^F}|.$$

From (2.21) and (2.22) we deduce that asymptotically in the model problem the most effective local radiating boundary condition is given by \mathfrak{B}_2^V , the second variable coefficient approximation in (2.10). At normal incidence, \mathfrak{B}_1^V is also more effective than either the first or second approximation from the frozen coefficient theory, but in general the second frozen coefficient approximation is superior to either of the first approximations. The numerical experiments in Section 6 confirm for general inhomogeneous media that \mathfrak{B}_2^V is significantly more effective than any of the other local radiating boundary conditions.

3. Radiating Boundary Conditions for Elastic Waves

Here we develop radiating boundary conditions for the elastic wave equation. Numerical calculation using this type of radiating boundary condition for elastic waves have already been reported in [2]. Our objective is to present a systematic derivation of a large class of radiating boundary conditions by using the approach developed in [4] and used throughout this paper.

The model problem which we must approximate has a solution u given by

$$(3.1) \quad \begin{aligned} \mathcal{L}u &= 0, & x > 0, & \quad t > 0, \\ u|_{x=0} &= g, \\ u &\text{ vanishes for } t < 0. \end{aligned}$$

Here $g = \begin{pmatrix} g_1 \\ g_2 \end{pmatrix}$ is a square integrable source function, $u = \begin{pmatrix} u_1 \\ u_2 \end{pmatrix}$ is a vector representing the x and y displacements, and \mathcal{L} is the elastic wave equation

$$(3.2) \quad \mathcal{L}u = \left[\begin{pmatrix} d_1 & 0 \\ 0 & d_2 \end{pmatrix} u_{xx} + \begin{pmatrix} 0 & d_1 - d_2 \\ d_1 - d_2 & 0 \end{pmatrix} u_{xy} + \begin{pmatrix} d_2 & 0 \\ 0 & d_1 \end{pmatrix} u_{yy} \right] - u_{tt},$$

where $d_1 = \lambda + 2\mu$, $d_2 = \mu$, λ and μ being the Lamé parameters. As the reader shall see below, we have used the (clamped) Dirichlet boundary conditions at $x=0$ rather than the normal stress condition because the explicit solutions from (3.1) are simpler to analyse. We design local radiation boundary conditions \mathcal{B} on $x=a$ so that if v satisfies

$$(3.3) \quad \begin{aligned} \mathcal{L}v &= 0, \\ v|_{x=0} &= g, \\ \mathcal{B}v|_{x=a} &= 0, \\ v &\text{ vanishes for } t < 0, \end{aligned}$$

then $v - u = \delta$, where δ is an acceptable error.

The non-local theoretical radiating boundary condition. As in Section 1, we use the Laplace transform to construct the solution u in (3.1). For s with $\Re s \geq 0$ and ω real, the operator \mathcal{L} has symbol

$$(3.4) \quad M(K, s, \omega) \equiv \begin{pmatrix} d_1 K^2 - d_2 \omega^2 - s^2 & (d_1 - d_2) i \omega K \\ (d_1 - d_2) i \omega K & d_2 K^2 - d_1 \omega^2 - s^2 \end{pmatrix}.$$

Given s with $\Re s \geq 0$, there are two distinct roots K_s^+ , K_p^+ with $\Re K_s^+ < 0$, $\Re K_p^+ < 0$ satisfying

$$(3.5) \quad \det(M(K, s, \omega)) = 0.$$

These roots have associated right eigenvectors $e_s^+(s, \omega)$, $e_p^+(s, \omega)$, bounded,

analytic, and linearly independent for $\Re s \geq 0$ satisfying

$$(3.6) \quad \begin{aligned} M(K_s^+, s, \omega) e_s^+ &= 0, \\ M(K_p^+, s, \omega) e_p^+ &= 0, \end{aligned}$$

and also left eigenvectors ${}^*e_s^+, {}^*e_p^+$, analytic functions of \bar{s} for $\Re s > 0$ with

$$(3.7) \quad {}^*e_i^+ \cdot e_j^+ = \delta_{i,j} \quad \text{for } i, j = s \text{ or } p.$$

Using these eigenvalues and eigenvectors, as in Section 1, we set $i\xi = \lim_{\eta \rightarrow 0, \eta > 0} (s = i\xi + \eta)$ and compute that the solution u in (3.1) is given by

$$(3.8) \quad \begin{aligned} u(x, y, t) = & \iint \exp \{K_s^+ x + i\xi t + i\omega y\} (\hat{g} \cdot {}^*e_s^+) e_s^+(\xi, \omega) d\xi d\omega \\ & + \iint \exp \{K_p^+ x + i\xi t + i\omega y\} (\hat{g} \cdot {}^*e_p^+) e_p^+(\xi, \omega) d\xi d\omega, \end{aligned}$$

where $K_j^+(\xi, \omega) = \lim_{\eta \rightarrow 0} K_j^+(s, \omega)$, etc. One calculates using (3.8) that u satisfies exactly the two *non-local perfectly radiating* boundary condition on $x = a$ given by

$$(3.9) \quad \begin{aligned} {}^*e_s^+ \cdot \left(\frac{d\hat{u}}{dx} - K_s^+(\xi, \omega) \right) \hat{u} \Big|_{x=a} &= 0, \\ {}^*e_p^+ \cdot \left(\frac{d\hat{u}}{dx} - K_p^+(\xi, \omega) \right) \hat{u} \Big|_{x=a} &= 0. \end{aligned}$$

Approximate radiating boundary conditions. Next we develop first- and second-order local approximate radiating boundary conditions by approximating the eigenvectors and eigenfunctions in (3.9) by rational functions of ω/ξ —thus, we approximate around normal incidence where $\omega/\xi = 0$. In contrast to the scalar wave equation treated in Section 1, there is an even larger number of ways to build these approximations and the authors have not been able to devise a systematic theoretical algorithm for generating stable local radiating boundary conditions. However, the numerical experiments in [2] provide convincing evidence for the utility of these boundary conditions.

One calculates that

$$(3.10) \quad \begin{aligned} \det(M(K, s, \omega)) = & d_1 d_2 K^4 - ((d_1^2 + d_2^2 - (d_1 - d_2)^2) \omega^2 + (d_1 + d_2) s^2) K^2 \\ & + (d_2 \omega^2 + s^2)(d_1 \omega^2 + s^2) = 0, \end{aligned}$$

so that, near normal incidence, the roots K_s^+ and K_p^+ have the expansions in

Taylor series given by

$$(3.11) \quad \begin{aligned} K_s^+(\xi, \omega) &= \frac{-i\xi}{\sqrt{d_2}} \left(1 - \frac{1}{2} \frac{\omega^2}{\xi^2} d_2 + O\left(\left|\frac{\omega}{\xi}\right|^4\right) \right), \\ K_p^+(\xi, \omega) &= \frac{-i\xi}{\sqrt{d_1}} \left(1 - \frac{1}{2} \frac{\omega^2}{\xi^2} d_1 + O\left(\left|\frac{\omega}{\xi}\right|^4\right) \right). \end{aligned}$$

We remark that, to the order given in (3.11), this Taylor expansion procedure is identical to the continued fraction expansions in Section 1. Near $\omega/\xi = 0$, the right eigenvectors are given by

$$(3.12) \quad \begin{aligned} e_s^+(s, \omega) &= \left(\frac{(d_2 - d_1)i\omega K_s^+}{d_1(K_s^+)^2 - d_2\omega^2 - s^2}, 1 \right), \\ e_p^+(s, \omega) &= \left(1, \frac{(d_2 - d_1)i\omega K_p^+}{d_2(K_p^+)^2 - d_1\omega^2 - s^2} \right), \end{aligned}$$

so nonzero multiples of the vectors ${}^*e_s^+, {}^*e_p^+$ are given by

$$(3.13) \quad \begin{aligned} \lambda_1 {}^*e_s^+ &= \left(\frac{(d_2 - d_1)i\omega \bar{K}_p^+}{d_2 \bar{K}_p^{+2} - d_1\omega^2 - \bar{s}^2}, 1 \right), \\ \lambda_2 {}^*e_p^+ &= \left(1, \frac{(d_2 - d_1)i\omega \bar{K}_s^+}{d_1 \bar{K}_s^{+2} - d_2\omega^2 - \bar{s}^2} \right), \end{aligned}$$

where $\lambda_1, \lambda_2 \neq 0$. Using the expansions in (3.11) we obtain

$$(3.14) \quad \begin{aligned} \lambda_1 {}^*e_s^+ &= \left(\sqrt{d_1} \frac{i\omega}{i\xi} + O\left(\left|\frac{\omega}{\xi}\right|^3\right), 1 \right), \\ \lambda_2 {}^*e_p^+ &= \left(1, -\sqrt{d_2} \frac{i\omega}{i\xi} + O\left(\left|\frac{\omega}{\xi}\right|^3\right) \right). \end{aligned}$$

Thus, the exact theoretical boundary condition from (3.9) can be approximated within $O(|\omega/\xi|^3)$ by

$$(3.15) \quad \left(1 + A_{-1} \left(\frac{i\omega}{i\xi} \right) \right) \frac{d\hat{v}}{dx} + i\xi \left(A_0 + A_1 \left(\frac{i\omega}{i\xi} \right) + A_2 \left(\frac{i\omega}{i\xi} \right)^2 \right) \hat{v} \Big|_{x=a} = 0,$$

where

$$(3.16) \quad \begin{aligned} A_{-1} &= \begin{pmatrix} 0 & -\sqrt{d_2} \\ \sqrt{d_1} & 0 \end{pmatrix}, & A_0 &= \begin{pmatrix} 1/\sqrt{d_1} & 0 \\ 0 & 1/\sqrt{d_2} \end{pmatrix}, \\ A_1 &= \begin{pmatrix} 0 & -\sqrt{d_2}/d_1 \\ \sqrt{d_1}/d_2 & 0 \end{pmatrix}, & A_2 &= \begin{pmatrix} -\frac{1}{2}\sqrt{d_1} & 0 \\ 0 & -\frac{1}{2}\sqrt{d_2} \end{pmatrix}. \end{aligned}$$

Given (3.16) we deduce that the first approximate local radiating boundary condition \mathcal{B}_1 is given by

$$(3.17) \quad \mathcal{B}_1 v \equiv \begin{aligned} & \frac{\partial v_1}{\partial x} + \frac{1}{\sqrt{d_1}} \frac{\partial v_1}{\partial t} \Big|_{x=a} = 0, \\ & \frac{\partial v_2}{\partial x} + \frac{1}{\sqrt{d_2}} \frac{\partial v_2}{\partial t} \Big|_{x=a} = 0. \end{aligned}$$

Using (3.15), we can also develop a large number of second-order radiating boundary condition \mathcal{B}_2^a , where \mathcal{B}_2^0 is defined by clearing the denominator in (3.15) itself resulting in

$$(3.18) \quad \mathcal{B}_2^0(v) \equiv \left(\frac{\partial^2}{\partial x \partial t} + A_{-1} \frac{\partial^2}{\partial x \partial y} + A_0 \frac{\partial^2}{\partial t^2} + A_1 \frac{\partial^2}{\partial t \partial y} + A_2 \frac{\partial^2}{\partial y^2} \right) v \Big|_{x=a} = 0.$$

This approximation contains the term $A_{-1} \partial^2 / \partial x \partial y$ which is difficult to difference in a stable fashion at the boundary. One way to avoid this difficulty is to use the elastic wave equation (3.2) and solve for v_{xy} in terms of v_{tt} , v_{xx} , and v_{yy} —this method has the disadvantage of introducing v_{xx} into the boundary conditions so that the discrete boundary conditions must be differenced at least one level further into the interior to maintain the same accuracy. A second method which eliminates the v_{xy} term but keeps the error to $O(|\omega/\xi|^3)$ is to make the “ansatz” for a radiating boundary condition with symbol of the form

$$(3.19) \quad \left(\frac{d}{dx} + i\xi \left(A_0 + \tilde{A}_1 \left(\frac{i\omega}{i\xi} \right) + \tilde{A}_2 \left(\frac{i\omega}{i\xi} \right)^2 \right) \right) \hat{v} \Big|_{x=a} = 0,$$

and to require that (3.19) agree with (3.15) to $O(|\omega/\xi|^3)$. Following this procedure, we arrive at a second-order local radiating boundary condition given by

$$(3.20) \quad \mathcal{B}_2^1 v|_{x=a} = \left(\frac{\partial^2}{\partial x \partial t} + A_0 \frac{\partial^2}{\partial t^2} + \tilde{A}_1 \frac{\partial^2}{\partial y \partial t} + \tilde{A}_2 \frac{\partial^2}{\partial y^2} \right) v \Big|_{x=a} = 0,$$

where \tilde{A}_1 and \tilde{A}_2 are calculated to be

$$(3.21) \quad \begin{aligned} \tilde{A}_1 &= (A_1 - A_{-1}A_0) = \begin{pmatrix} 0 & (\sqrt{d_1} - \sqrt{d_2})/\sqrt{d_1} \\ (\sqrt{d_1} - \sqrt{d_2})/\sqrt{d_2} & 0 \end{pmatrix}, \\ \tilde{A}_2 &= (A_{-1})^2 A_0 - A_{-1}A_1 + A_2 = \begin{pmatrix} \frac{1}{2}\sqrt{d_1} - \sqrt{d_2} & 0 \\ 0 & \frac{1}{2}\sqrt{d_2} - \sqrt{d_1} \end{pmatrix}. \end{aligned}$$

The radiating boundary condition (3.20) with coefficients determined in (3.21) is the boundary condition used in the numerical calculations in [2].

Similarly, more general second-order approximations \mathcal{B}_2^α can be defined by writing (3.15) as

$$\left(1 + A_{-1}\left(\frac{i\omega}{i\xi}\right)\right)^{1-\alpha} \frac{d\hat{v}}{dx} + \left(1 + A_{-1}\left(\frac{i\omega}{i\xi}\right)\right)^{-\alpha} i\xi \left(A_0 + A_1\left(\frac{i\omega}{i\xi}\right) + A_2\left(\frac{i\omega}{i\xi}\right)^2\right) \hat{v} \Big|_{x=a} = 0,$$

and then using the above procedure to match coefficients. It is clear that among the \mathcal{B}_2^α only \mathcal{B}_2^1 contains no v_{xy} term.

4. Radiation Boundary Conditions at Corners

In many practical seismic and acoustic calculations, radiation boundary conditions are needed in regions with corners. If the higher-order radiation boundary conditions discussed in the preceding sections are implemented in a careless fashion, numerical calculations indicate that the corners act as point sources and create instabilities. Here we give a brief discussion of some strategies at corners which have proven effective both for acoustic and elastic wave calculations—the corresponding difference formulae in these cases are displayed in Appendix B.

For simplicity in exposition, we concentrate here on the model corner problem

$$(4.1) \quad \frac{\partial^2 u}{\partial t^2} - \frac{\partial^2 u}{\partial x^2} - \frac{\partial^2 u}{\partial y^2} = 0 \quad \text{in } x \geq 0, y \geq 0,$$

$$\mathcal{B}_1 u \Big|_{\substack{x=0 \\ y \geq 0}} = 0,$$

$$\mathcal{B}_2 u \Big|_{\substack{y=0 \\ x \geq 0}} = 0.$$

In the seismic model discussed in the introduction, the surface $x=0$ can represent a physical boundary so that the Neumann boundary condition, $\mathcal{B}_1 \equiv \partial/\partial x$, is appropriate or this surface may represent an artificial computational boundary where a radiation boundary condition is necessary. Below, we assume that both of the walls require radiation boundary conditions although all remarks have obvious analogues in the other case.

Some theoretical remarks on radiation conditions and corners. Naively, following the guidelines from [4] and the previous sections, one might choose

\mathcal{B}_1 and \mathcal{B}_2 in (4.1) to be given through the second-order approximations in (1.5) by

$$(4.2) \quad \begin{aligned} \mathcal{B}_1 u &\equiv \frac{\partial^2 u}{\partial t^2} - \frac{\partial^2 u}{\partial t \partial x} - \frac{1}{2} \frac{\partial^2 u}{\partial y^2} \Big|_{\substack{x=0 \\ y \geq 0}} = 0, \\ \mathcal{B}_2 u &\equiv \frac{\partial^2 u}{\partial t^2} - \frac{\partial^2 u}{\partial t \partial y} - \frac{1}{2} \frac{\partial^2 u}{\partial x^2} \Big|_{\substack{y=0 \\ x \geq 0}} = 0. \end{aligned}$$

The choice of the two boundary conditions in (4.2) effectively reduces the artificial reflection of waves away from the corner; however, \mathcal{B}_1 involves second derivatives along the boundary in y while \mathcal{B}_2 involves second derivatives along the boundary in x and practically it is not obvious how to match the discrete versions of the boundary conditions at the corner grid points. Furthermore, numerical experiments indicate that a careless use of the boundary conditions in (4.2) generates instabilities.

On the other hand, if one chooses \mathcal{B}_1 and \mathcal{B}_2 in (4.1) to be given by the first-order approximations from (1.5) as

$$(4.3) \quad \begin{aligned} \mathcal{B}_1 u &\equiv \left(\frac{\partial}{\partial t} - \frac{\partial}{\partial x} \right) u \Big|_{\substack{x=0 \\ y \geq 0}} = 0, \\ \mathcal{B}_2 u &\equiv \left(\frac{\partial}{\partial t} - \frac{\partial}{\partial y} \right) u \Big|_{\substack{y=0 \\ x \geq 0}} = 0, \end{aligned}$$

then a trivial application of the standard energy identity for the wave equation

$$\frac{\partial}{\partial t} \int_{\Omega} \frac{1}{2} (u_t^2 + |\nabla u|^2) dx = \int_{\partial\Omega} u_t \frac{\partial u}{\partial n} ds$$

establishes the fact that the boundary conditions in (4.3) are well-posed at the corner. Furthermore, the discrete version of \mathcal{B}_1 involves no y differences while the discrete version of \mathcal{B}_2 involves no x differences; thus the two boundary conditions are easily matched at the corner. Nevertheless, away from the corner, the boundary conditions in (4.3) produce significantly larger reflected waves than the boundary conditions in (4.2).

It is apparent that the simplest theoretical choice of the boundary conditions \mathcal{B}_1 and \mathcal{B}_2 which retains the practical advantages of both types of boundary conditions is to choose boundary conditions behaving like (4.2) away from the corner and like (4.3) in the vicinity of the corner. We observe

that the boundary conditions in (4.2) can be written (and used!!) just as effectively in the time-integrated form

$$\left. \frac{\partial u}{\partial t} - \frac{\partial u}{\partial x} + \frac{1}{2} \frac{\partial^2}{\partial y^2} \left(\int_0^t u \, d\tau \right) \right|_{\substack{x=0 \\ y \geq 0}} = 0,$$

$$\left. \frac{\partial u}{\partial t} - \frac{\partial u}{\partial y} + \frac{1}{2} \frac{\partial^2}{\partial x^2} \left(\int_0^t u \, d\tau \right) \right|_{\substack{y=0 \\ x \geq 0}} = 0.$$

Next, we choose $a \in C^\infty(R^1)$ so that $a \geq 0$, $a(s) \equiv 1$ for $s > 1$, $a(s) \equiv 0$ for $s \leq \frac{1}{2}$ and set $a_\varepsilon(s) = a(s/\varepsilon)$ for any $\varepsilon > 0$. We define the analytic second-order radiating boundary conditions for the problem in (4.1) by

$$(4.4) \quad \mathcal{B}_1 u \equiv \frac{\partial u}{\partial t} - \frac{\partial u}{\partial x} + \frac{1}{2} a_\varepsilon(y) \frac{\partial^2}{\partial y^2} \left(\int_0^t u \, d\tau \right) \Big|_{\substack{x=0 \\ y \geq 0}} = 0,$$

$$\mathcal{B}_2 u \equiv \frac{\partial u}{\partial t} - \frac{\partial u}{\partial y} + \frac{1}{2} a_\varepsilon(x) \frac{\partial^2}{\partial x^2} \left(\int_0^t u \, d\tau \right) \Big|_{\substack{y=0 \\ x \geq 0}} = 0.$$

By combining finite propagation speed, the energy estimate near the corner for the boundary conditions in (4.3), and the well-posedness of the boundary conditions in (4.2) established in Section 1, we easily deduce

PROPOSITION 4.1. *The boundary conditions \mathcal{B}_1 and \mathcal{B}_2 defined in (4.4) are stable radiating boundary conditions for the wave equation in the corner region $x \geq 0, y \geq 0$.*

Some practical strategies for radiating boundary conditions in corners. In the preceding theoretical discussion, the parameter ε in (4.4) was left undetermined. In the numerical calculations we have observed that we do not need a gradual transition region where the second-order approximate boundary condition is smoothly deformed to a first-order condition. In fact the *higher-order approximation can be used for all boundary mesh points except the corner and the two closest boundary grid points* so that ε is the spatial step size in practice.

We find it convenient to rotate the boundary condition so that it is exact for plane waves travelling in the direction of the bisector at the corner. This approach can be used in the difference approximation for both the acoustic and elastic wave equations. Using this strategy, the analytic corner condition

for (4.1) to be approximated at the corner mesh point and the two closest boundary points is

$$(4.5) \quad \left(\sqrt{2} \frac{\partial}{\partial t} - \frac{\partial}{\partial x} - \frac{\partial}{\partial y} \right) u \Big|_{\substack{x=0 \\ y=0}} = 0.$$

See Appendix B for the explicit form of the difference formulae.

We have also tested some other corner strategies which do not give rise to instabilities. All of them have similar behavior regarding reflections.

For example, it is possible to apply the corner condition (4.5) only at one grid point. The higher-order approximations for the points adjacent to the corner will then be coupled. A small system of linear equations must be solved. Another possibility is to use a first-order radiation boundary condition which is exact for plane waves travelling in the direction of the mesh diagonal. In this case, the difference approximation only involves points along the mesh diagonal.

5. Radiation Boundary Conditions for the Difference Equation

In order to derive radiation boundary conditions for the approximating difference equation we have first determined the corresponding conditions for the continuous problem, then these conditions have been discretized. In this way the difference formula used in the interior does not effect the design of the boundary conditions except for stability considerations.

The approach works well if the interior truncation errors are small and hence the solution of the differential equation and its corresponding difference approximation are close. If, on the other hand, essential parts of the solution contain frequencies that are described with only a few points per wave length, it is better to design a discrete radiation condition directly for the difference equation.

Derivation of discrete radiation conditions. The discrete radiation condition can be derived in analogy with the procedure for the continuous problem. This will be an improvement as compared to the use of approximations of high numerical order to the continuous boundary conditions. However, in general the result will be considerably more complex. We shall concentrate on an example where the analytic theory is trivial because a *local* perfectly absorbing boundary condition exists but where we need a nonlocal condition for the corresponding difference approximation.

We consider the scalar wave equation in one space dimension

$$(5.1) \quad \left(\frac{\partial^2}{\partial t^2} - \frac{\partial^2}{\partial x^2} \right) u(x, t) = 0, \quad x, t > 0,$$

and the explicit difference approximations

$$(5.2) \quad L_{\Delta} u_j^n = (D_+^t D_-^t - D_+^x D_-^x) u_j^n = 0, \quad n, j \geq 1.$$

Here the mesh function u_j^n approximates $u(x_j, t^n)$ on the grid (x_j, t^n) , $j = 0, 1, \dots, n = 0, 1, \dots$, $x_j = j\Delta x$, $t^n = n\Delta t$. The operators D_+ and D_- denote forward and backward divided differences, respectively. For example,

$$D_+^t u_j^n = (u_j^{n+1} - u_j^n) / \Delta t.$$

We assume that $\Delta t < \Delta x$ which guarantees stability of the Cauchy problem.

We recall that the perfectly absorbing boundary condition for (5.1) at $x = 0$ is local and very simple:

$$(5.3) \quad \left(\frac{\partial}{\partial t} - \frac{\partial}{\partial x} \right) u \Big|_{x=0} = 0.$$

The difference equation (5.2) does not have a local perfectly absorbing boundary condition. On the other hand, we shall construct better absorbing boundary conditions than just high-order approximation of (5.3).

The symbol of the difference operator L_{Δ} in (5.2) is

$$(5.4) \quad \hat{L}_{\Delta}(\omega, \xi) = -\frac{4}{\Delta t^2} (\sin \tfrac{1}{2} \xi \Delta t)^2 + \frac{4}{\Delta x^2} (\sin \tfrac{1}{2} \omega \Delta x)^2,$$

where ω and ξ are the x and t duals, respectively,

$$(5.5) \quad \hat{L}_{\Delta}(\omega, \xi) = \left(\frac{2i}{\Delta t} \sin \tfrac{1}{2} \xi \Delta t + \frac{2i}{\Delta x} \sin \tfrac{1}{2} \omega \Delta x \right) \left(\frac{2i}{\Delta t} \sin \tfrac{1}{2} \xi \Delta t - \frac{2i}{\Delta x} \sin \tfrac{1}{2} \omega \Delta t \right).$$

The second factor describes outgoing waves and will be the symbol of our theoretical discrete radiation boundary condition at $x = 0$. This means that we would like to have a difference equation at $j = 0$ which has a dispersion relation given by

$$(5.6) \quad \frac{2i}{\Delta t} \sin \tfrac{1}{2} \xi \Delta t - \frac{2i}{\Delta x} \sin \tfrac{1}{2} \omega \Delta x = 0.$$

This relation differs from the dispersion relation of the continuous boundary condition in (5.3).

Equation (5.6) is not directly realizable on the grid. It can be written as

$$(5.7) \quad \exp\{\tfrac{1}{2}i\xi\Delta t\} - \exp\{-\tfrac{1}{2}i\xi\Delta t\} - \frac{\Delta t}{\Delta x} (\exp\{\tfrac{1}{2}i\omega\Delta x\} - \exp\{-\tfrac{1}{2}i\omega\Delta x\}) = 0$$

and this symbol corresponds to a difference stencil where the mesh points should be half steps ($\frac{1}{2}\Delta x$ and $\frac{1}{2}\Delta t$) away from some point (\bar{x}, \bar{t}) in both the x and t directions. This theoretical discrete boundary condition cannot be realized as an operator involving a finite number of points on the original grid. We can however produce (5.6) as the dispersion relation of an operator involving infinitely many points of the grid by using the identities ($\alpha \neq \pm\pi$)

$$(5.8) \quad \begin{aligned} 2i \sin \tfrac{1}{2}\alpha &= \frac{2i \sin \tfrac{1}{2}\alpha \cos \tfrac{1}{2}\alpha}{(1 - \sin^2 \tfrac{1}{2}\alpha)^{1/2}} = \frac{i \sin \alpha}{(1 - \sin^2 \tfrac{1}{2}\alpha)^{1/2}} \\ &= i \sin \alpha \left(1 + \tfrac{1}{2} \sin^2 \tfrac{1}{2}\alpha + \frac{1 \cdot 3}{2 \cdot 4} \sin^4 \tfrac{1}{2}\alpha + \cdots \right). \end{aligned}$$

Formula (5.9) below gives a representation of a pseudodifference operator which has the dispersion relation (5.6):

$$(5.9) \quad \begin{aligned} D_0^t \left(1 - \tfrac{1}{2}(\tfrac{1}{4}\Delta t^2 D_+^t D_-^t) + \frac{1 \cdot 3}{2 \cdot 4} (\tfrac{1}{4}\Delta t^2 D_+^t D_-^t)^2 - \cdots \right) \\ - D_0^x \left(1 - \tfrac{1}{2}(\tfrac{1}{4}\Delta x^2 D_+^x D_-^x) + \frac{1 \cdot 3}{2 \cdot 4} (\tfrac{1}{4}\Delta x^2 D_+^x D_-^x)^2 - \cdots \right). \end{aligned}$$

Here D_0 denotes the centered difference ($D_0 = \frac{1}{2}(D_+ + D_-)$).

Approximate discrete radiating conditions. The operator (5.9) is not unique in the sense that there are many ways of representing the function $\sin(\frac{1}{2}\xi\Delta t)$ with expressions that are duals of difference operators on the rectangular grid.

Another way of deriving asymptotic radiation difference operators is using interpolation. The desired function values in between the grid points are represented via interpolation on the grid. For example we can use forward and backward Newton interpolation in the x and t directions, respectively, to produce the boundary condition

$$(5.10) \quad \left(\left(1 + \sum_{j=1}^J \binom{\frac{1}{2}-j}{j} (\Delta t D_-^t) \right) D_-^t - \left(1 + \sum_{j=1}^J \binom{-\frac{1}{2}}{j} (\Delta x D_+^x) \right) D_+^x \right) u_0^{n+1} = 0.$$

Instead of picking the first terms in some representation of the perfectly absorbing boundary condition, we can take a more computationally oriented approach. A certain practical form of the boundary operator is assumed in advance. The coefficients are then determined in such a way that the method is stable and its symbol approximates (5.6) well.

We shall use a linear combination of the values u_1^{n+1} , u_0^n , u_1^n , u_0^{n-1} and u_1^{n-1} for determining the boundary value u_0^{n+1} . (Given the form of the interior difference scheme in (5.2) this is a practical constraint.) We study discrete radiation boundary conditions of the form

$$(5.11) \quad D_0^x \left(\frac{u_0^n + u_1^n}{2} \right) - \theta D_+^x u_0^n - (1 - \theta) D_+^x \left(\frac{u_0^{n+1} + u_0^{n-1}}{2} \right) = 0.$$

Here θ is a real parameter. This class of boundary conditions is at least a second-order approximation of (5.3) for any choice of θ and involves the appropriate grid points.

We get the local truncation error T by letting the operator in (5.11) act on a smooth function and cancelling the leading term using (5.3). The result at the point $(t^n, x_{1/2})$ is

$$(5.12) \quad T = \Delta t^2 \left(\frac{1}{6} \frac{\partial^3 u}{\partial t^3} - \frac{1}{2} (1 - \theta) \frac{\partial^3 u}{\partial x \partial t^2} \right) + \Delta x^2 \left(\frac{1}{8} \frac{\partial^3 u}{\partial t \partial x^2} - \frac{1}{24} \frac{\partial^3 u}{\partial x^3} \right) + O(\Delta t^4 + \Delta x^4).$$

The dispersion relation is

$$\frac{i \sin \xi \Delta t}{\Delta t} (\cos \frac{1}{2} \omega \Delta x) - \frac{2\theta i}{\Delta x} \sin \frac{1}{2} \omega \Delta x - \frac{2(1-\theta)i}{\Delta x} \sin \frac{1}{2} \omega \Delta x \cos \xi \Delta t = 0,$$

which can be simplified to

$$(5.13) \quad \sin \xi \Delta t - 2\theta \lambda \tan \frac{1}{2} \omega \Delta x - 2(1 - \theta) \tan \frac{1}{2} \omega \Delta x \cos \xi \Delta t = 0,$$

where $\lambda = \Delta t / \Delta x$.

One possible strategy for choosing θ is to maximize the order of the truncation error (5.12). Using (5.3) the truncation error can be written as

$$(5.14) \quad T = (\Delta t^2 (\frac{1}{6} - \frac{1}{2}(1 - \theta)) + \Delta x^2 (\frac{1}{8} - \frac{1}{24})) \frac{\partial^3 u}{\partial t^3} + O(\Delta t^4 + \Delta x^4).$$

The second-order terms vanish for

$$(5.15) \quad \theta = \frac{4\lambda^2 - 1}{6\lambda^2}$$

and, with this choice of θ , (5.11) is an approximation of (5.3) of fourth order. This procedure is equivalent to matching (5.13) to the dispersion relation of (5.3) modulo terms of fourth order in Δx and Δt .

In the direct discrete approach, θ is determined in such a way that the dispersion relation (5.13) is as good an approximation of (5.6) as possible. If we expand the trigonometric functions in Taylor series, all error terms of Δx and Δt up to fourth order can be annihilated if θ is chosen as

$$(5.16) \quad \theta = \frac{3\lambda^2 - 1}{4\lambda^2}.$$

In analogy with the continuous case, we determine the reflection coefficient R by applying the boundary condition to the solution of the interior difference equation in (5.2) given by

$$(5.17) \quad u_j^n = \exp \{i(\xi \Delta t n + \omega \Delta x j)\} + R \exp \{i(\xi \Delta t n - \omega \Delta x j)\},$$

with

$$\sin \frac{1}{2} \xi \Delta t = \lambda \sin \frac{1}{2} \omega \Delta x,$$

and requiring that u_j^n satisfy the discrete boundary conditions exactly. If $D(\xi \Delta t, \omega \Delta x)$ is the symbol of the boundary operator, the explicit form of the reflection coefficient is

$$(5.18) \quad R = \frac{D(\xi \Delta t, \omega \Delta x)}{D(\xi \Delta t, -\omega \Delta x)}$$

with

$$\begin{aligned} \sin \frac{1}{2} \xi \Delta t &= \lambda \sin \frac{1}{2} \omega \Delta x, \\ -\pi &\leq \xi, \omega \leq \pi. \end{aligned}$$

When θ is given by (5.15), $R = O((\omega \Delta x)^2)$ and when θ is determined from (5.16), $R = O((\omega \Delta x)^4)$.

In Figures 5.1 and 5.2 the absolute value of the reflection coefficient R is displayed as a function of the wave number $\omega \Delta x$. The reflections from scheme

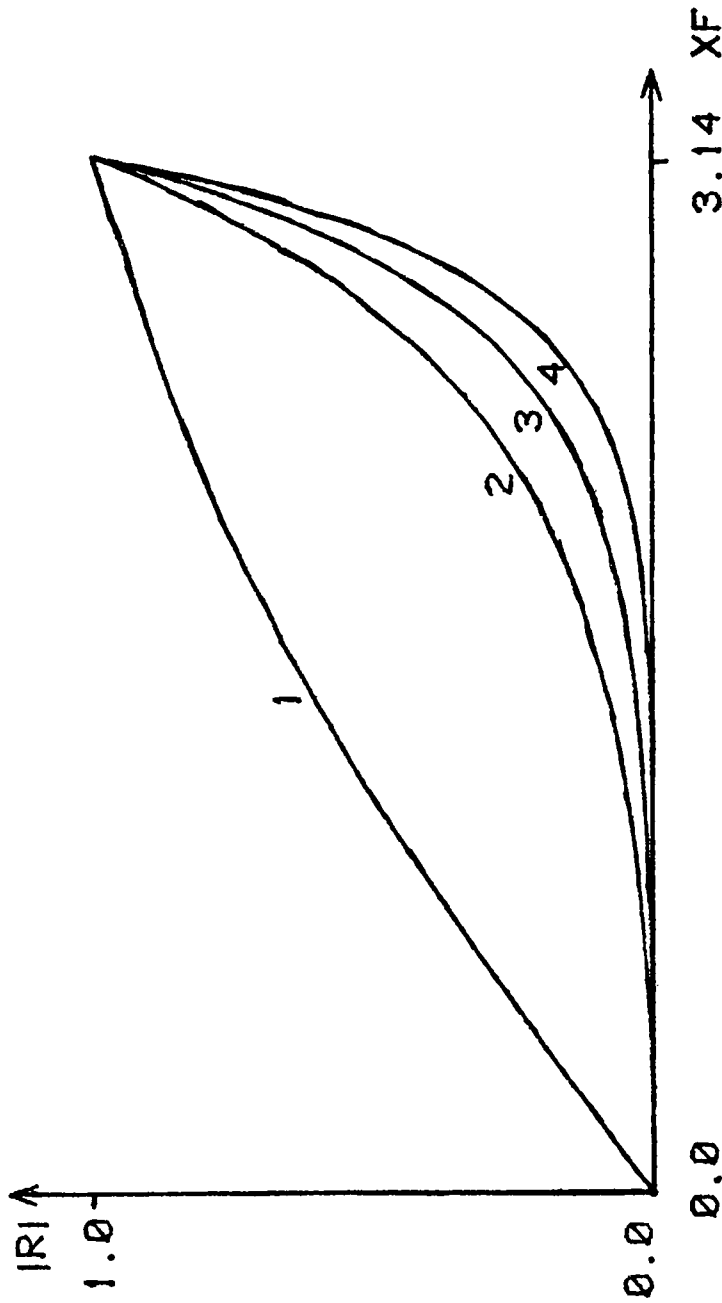


Figure 5.1. Absolute value of the reflection coefficient ($|R|$) as a function of $XF = \omega\Delta x$. Curve 1: Method (5.19), first-order; curve 2: (5.20), second-order; curve 3: (5.11), fourth-order analytic $\theta = (4\lambda^2 - 1)/6\lambda^2$; curve 4: (5.11), fourth-order discrete $\theta = (3\lambda^2 - 1)/4\lambda^2$, $\lambda = 0.75$.

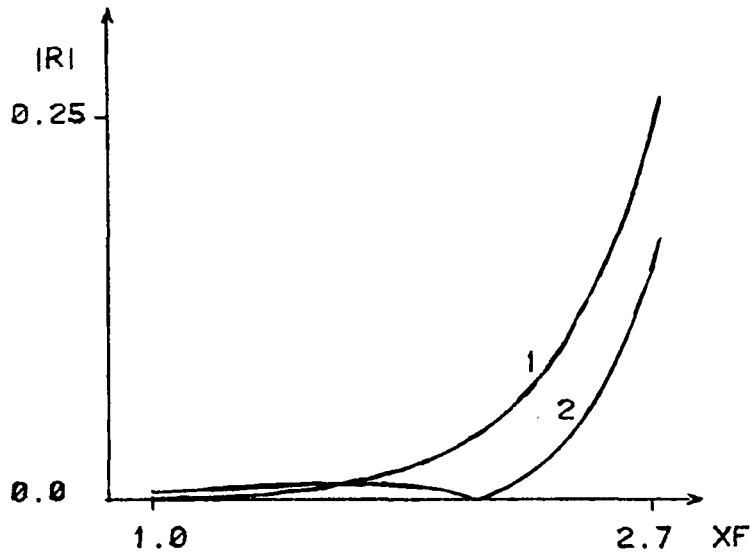


Figure 5.2. Absolute value of the reflection coefficient ($|R|$) as a function of $XF = \omega \Delta x$. Curve 1: Method (5.11), fourth-order discrete $\theta = 0.31$; curve 2: (5.11), $\theta = 0.27$.

(5.11) is compared to reflections when using the simpler boundary conditions

$$(5.19) \quad (D'_- - D^*_+)u_0^{n+1} = 0,$$

$$(5.20) \quad D'_+\left(\frac{u_0^n + u_1^n}{2}\right) - D^*_+\left(\frac{u_0^n + u_0^{n+1}}{2}\right) = 0.$$

All these boundary approximations are consistent with the analytic radiation boundary condition (5.3). The scheme (5.19) is a first-order numerical approximation and produces by far the largest reflections. The box scheme (5.20) is of second order. Figure 5.1 shows the smallest reflections for the approximation (5.11) when $\theta = (3\lambda^2 - 1)/4\lambda^2$.

In Figure 5.2 this choice of θ is compared to one of the many other possible principles for determining θ : Choose θ in order to maximize α such that

$$\max_{0 \leq \omega \Delta x \leq \alpha} |R| \leq 0.01.$$

For $\lambda = 0.75$ we determine θ numerically to be 0.27.

Note that $\omega\Delta x = \pi$ corresponds to glancing and hence $|R| = 1$. These high frequency reflections are not particularly dangerous in practice, since these waves propagate slowly into the interior.

Explicit numerical calculations using the interior scheme (5.2) together with (5.11) at the boundary give results which agree with the reflection coefficient diagrams. If the analytic solution contains a fair amount of high frequencies, the difference in the approximations when determining θ via (5.15) and (5.16) is significant. For $u(x, t) = f(x + t - d_0)$, $d_0 > 0$, where

$$f(y) = \begin{cases} 0 & \text{for } |y - d| \geq d, \\ y/d & \text{for } 0 < y < d, \\ (2d - y)/d & \text{for } d < y < 2d, \end{cases}$$

and with the pulse spread over 5 mesh points the size of the reflections are given in Table 5.1. The solution on the half-bounded interval is compared to the discrete solution of the Cauchy problem.

Table 5.1
The l_2 norm of the reflected wave $\|u_R\|$ in percent of the l_2 norm of initial data after 25 time steps.

Boundary Condition:	(5.11)–(5.15)		(5.11)–(5.16)	
	$\ u_R\ $	θ	$\ u_R\ $	θ
$\lambda = 0.5$	1.72	0.00	0.54	-0.25
$\lambda = 0.75$	1.65	0.37	0.92	0.31

For large λ the truncation error in the interior approximation is small. Hence the difference between choosing θ from (5.15) and (5.16) is not so significant. The boundary condition (5.11) is a linear combination of mesh function values. When the scheme is normalized such that the factor in front of u_0^{n+1} equals one, then the absolute values of all other factors are bounded by one if

$$-1/2\lambda - 1 \leq \theta \leq 1/6\lambda + \frac{1}{3}.$$

This is also the stability limit which was observed in the calculations.

Discrete radiation conditions in two space dimensions. In more than one space dimension already the analytic radiation boundary condition for the scalar wave equation is nonlocal. Hence for the discrete boundary condition we need an approximation over a range of incident angles as in the analytic case but also over a range of wave numbers as for the discrete one-dimensional problem.

Let the wave equation

$$\left(\frac{\partial^2}{\partial t^2} - \left(\frac{\partial^2}{\partial x^2} + \frac{\partial^2}{\partial y^2}\right)\right)u(x, y, t) = 0, \quad x > 0,$$

be approximated in the interior by

$$(D_+^t D_-^t - (D_+^x D_-^x + D_+^y D_-^y))u_{jk}^n = 0,$$

where u_{jk}^n is an approximation of $u(x_j, y_k, t^n)$. The symbol of the difference operator is

$$-\frac{4}{\Delta t^2}(\sin \tfrac{1}{2}\xi \Delta t)^2 + \frac{4}{\Delta x^2}(\sin \tfrac{1}{2}\omega_x \Delta x)^2 + \frac{4}{\Delta y^2}(\sin \tfrac{1}{2}\omega_y \Delta y)^2.$$

Following the derivation in Section 1, we get the dispersion relation for outgoing discrete waves

$$(5.21) \quad \frac{1}{\Delta x} \sin \tfrac{1}{2}\omega_x \Delta x - \left(\frac{1}{\Delta t^2} (\sin \tfrac{1}{2}\xi \Delta t)^2 - \frac{1}{\Delta y^2} (\sin \tfrac{1}{2}\omega_y \Delta y)^2 \right)^{1/2} = 0.$$

Here we shall not analyse local realizations of (5.21) on the grid. A practical compromise is to approximate the second-order analytic boundary condition in (1.5) by differences but to treat the important terms $\partial^2 u / \partial t^2$ and $\partial^2 u / \partial t \partial x$ by following the one-dimensional discrete analysis sketched above.

6. A Variable Coefficient Numerical Case Study

The acoustic wave equation

$$(6.1) \quad \nu^2(x) \frac{\partial^2 u}{\partial t^2} - \frac{\partial^2 u}{\partial x^2} - \frac{\partial^2 u}{\partial y^2} = 0, \quad x > 0, t > 0,$$

$$(6.2) \quad \left. \frac{\partial u}{\partial x} \right|_{x=0} = 0,$$

is given with a variable index of refraction $\nu(x)$ and with Neumann boundary condition at $x = 0$.

The purpose of this section is to study a simple difference approximation of (6.1), (6.2) on the bounded domain $0 \leq x \leq a$, $-b \leq y \leq b$ with different radiation boundary conditions at $x = a$ and $y = \pm b$. Here we want to complement the conclusions from the asymptotic analysis in Section 2 by quantitative results from numerical test.

The solution of (6.1), (6.2) is approximated by the mesh function u_{jk}^n in $0 \leq x \leq a$, $-b \leq y \leq b$ on the grid (x_j, y_k, t^n) , $x_j = j\Delta x - \frac{1}{2}\Delta x$, $y_k = k\Delta y$, $t^n = n\Delta t$, $j = 0, 1, \dots, J$, $k = -K, -K+1, \dots, K$, $n = 0, 1, \dots$, $\Delta x = a/(J-0.5)$, $\Delta y = b/K$. The second-order explicit difference approximation

$$(6.3) \quad (\nu^2(x_j)D_+^t D_-^t - D_+^x D_-^x - D_+^y D_-^y)u_{j,k}^n = 0$$

is used in the interior $j = 1, 2, \dots, J-1$, $k = -K+1, \dots, K-1$, $n = 1, 2, \dots$. The boundary condition (6.2) is approximated by

$$(6.4) \quad D_+ u_{0,k}^n = 0, \quad k = -K, \dots, K, n = 1, 2, \dots$$

Initial values are given for $n = 0, 1$.

In our experiment the initial data and hence the solution is symmetric around $y = 0$; therefore, we perform the calculation only for positive y . The radiation boundary conditions at $y = -b$ are the same for $y = b$ if the signs of the y derivatives and the y differences are reversed.

The following boundary conditions at $x = a$ and $y = b$ are studied (consult Appendix B for the precise formulae):

$$(6.5) \quad \begin{aligned} & D_-^x u_{J,k}^n = 0, & k = 0, \dots, K, n = 0, 1, \dots, \\ & B_{\Delta 0}: & \\ & D_-^y u_{j,K}^n = 0, & j = 1, \dots, J-1, n = 0, 1, \dots, \\ & B_{\Delta 1}^F: & \text{equations (B.3) and (B.4) with } \nu_x = 0, \\ & B_{\Delta 2}^F: & \text{equations (B.1) and (B.2) with } \nu_x = \nu_{xx} = 0, \\ & B_{\Delta 1}^V: & \text{equations (B.3) and (B.4),} \\ & B_{\Delta 2}^V: & \text{equations (B.1) and (B.2).} \end{aligned}$$

At the corner points $(j, k) = (J, K-1)$, $(J-1, K)$ and (J, K) , formula (B.9) is applied for all cases but for $B_{\Delta 0}$. We use the Neumann condition $B_{\Delta 0}$ for reference. The equations $B_{\Delta 1}^F$ and $B_{\Delta 2}^F$ correspond to the frozen coefficient radiation condition of first and second order, respectively (see Section 2 and the appendix). The last equations $B_{\Delta 1}^V$ and $B_{\Delta 2}^V$ correspond to the variable coefficient radiation conditions.

A fairly smooth and expanding cylindrical wave pulse is given as initial data in the numerical tests:

$$(6.6) \quad \begin{aligned} u(x, y, 0) &= f((x^2 + y^2)^{1/2} - r_0), \\ u(x, y, \Delta t) &= f((x^2 + y^2)^{1/2} - r_0 - \Delta t/\nu(x)), \\ f(r) &= \begin{cases} 0 & \text{for } |r| \geq d, \\ \frac{1}{2}(\cos(\pi r/d) + 1) & \text{for } |r| < d. \end{cases} \end{aligned}$$

Three different indices of refraction (velocity profiles) are tested:

$$(6.7) \quad \begin{aligned} \nu_1: \nu(x) &= 1, \\ \nu_2: \nu(x)^{-1} &= \frac{1}{6}(5 - \cos(\pi x/a)), \\ \nu_3: \nu(x)^{-1} &= 1 - x/2a. \end{aligned}$$

The calculations on the bounded domain $0 \leq x \leq a$, $0 \leq y \leq b$ are compared with calculations on a larger domain $0 \leq x \leq 3a$, $0 \leq y \leq 3b$ in order to determine the reflections. The l_2 -norm of the reflections are given in Table 6.1 in percent of the l_2 -norm of the reflection when using $B_{\Delta 0}$. The result is displayed for $t = t_1$ when the pulse just has passed the boundary and for $t_2 = 2t_1$. The pulse spreads out over 12 grid points initially.

Table 6.1
Boundary reflections using radiation boundary conditions in percent of the reflection using the Neumann condition.

	ν_1		ν_2		ν_3	
	t_1	t_2	t_1	t_2	t_1	t_2
$B_{\Delta 1}^F$	7.26	10.44	3.03	6.30	2.24	6.13
$B_{\Delta 2}^F$	0.91	1.87	0.74	1.82	0.84	1.69
$B_{\Delta 1}^V$	7.26	10.44	3.01	6.30	2.16	6.07
$B_{\Delta 2}^V$	0.91	1.87	0.41	0.92	0.40	1.12

In each calculation the radiations boundary conditions reduce the reflections drastically compared to the Neumann condition. As expected from earlier experiments (cf. [2], [4]), the second-order methods are substantially better than the first-order ones. In the above experiments, the discrete second-order variable coefficient approximation $B_{\Delta 2}^V$ produces the smallest magnitudes of reflection and these are roughly one-half the magnitudes associated with the second-order frozen coefficient approximation $B_{\Delta 2}^F$. In general, variable coefficient schemes perform better than the corresponding frozen coefficient schemes but the improvement is modest. In our examples the variable coefficient term in the first-order scheme $B_{\Delta 1}^V$ has almost negligible effect. The frozen coefficient method $B_{\Delta 2}^F$ gives smaller reflections than $B_{\Delta 1}^V$. This is confirmed by the asymptotic analysis in Section 2. The experiments indicate that for our examples (with ν_2 and ν_3) roughly half of the reflection when using $B_{\Delta 2}^F$ depends on effects from the variable coefficients. The other half depends on large angles of incidence, evanescent waves or on insufficient resolution on the grid. The high numbers for the reflection with ν_1 depends on the fact that the velocity ν_1^{-1} is larger than ν_2^{-1} and ν_3^{-1} on

the average. More waves with angles closer to glancing and with high frequencies hit the boundary.

The size of the reflections are of course highly problem dependent. In different experiments we have gotten higher and lower values than those given in the table. The experiments and numbers presented are from our experience typical for these types of calculations.

Finally we mention that in mesh with random initial data all schemes showed a stable behavior.

Appendix A Derivation of the Variable Coefficient Theoretical Radiation Boundary Conditions

To illustrate the general procedure used to derive the variable coefficient theoretical radiation boundary conditions used in Sections 2 and 6, we develop this procedure for variable velocity wave equations of the form

$$(A.1) \quad \mathcal{L} = \nu^2(x) \frac{\partial^2}{\partial t^2} - \frac{\partial^2}{\partial x^2} - \frac{\partial^2}{\partial y^2}$$

and for the computational boundaries $x = a$ and $y = b$. (We assume that the index of refraction $\nu(x)$ is real and positive.)

Before proceeding with these calculations, we recall a few general facts about pseudo-differential operators (see Nirenberg's lectures [8]). If $b(\tilde{x}, \tilde{\xi})$ is an infinitely differentiable function, then $b(\tilde{x}, \tilde{\xi}) \in S^m$ provided there exists $C_{\alpha, \beta}$ such that

$$\left| \frac{\partial^\alpha}{\partial \tilde{x}^\alpha} \frac{\partial^\beta}{\partial \tilde{\xi}^\beta} b(\tilde{x}, \tilde{\xi}) \right| \leq C_{\alpha, \beta} (1 + |\tilde{\xi}|)^{m - |\beta|}.$$

Associated with any $b(\tilde{x}, \tilde{\xi}) \in S^m$ is a pseudo-differential operator $b(\tilde{x}, (1/i)\partial/\partial\tilde{x}) \in \text{OP}(S^m)$ defined via the fourier transform by

$$(A.2) \quad b\left(\tilde{x}, \frac{1}{i} \frac{\partial}{\partial \tilde{x}}\right) v = \int \exp\{i\tilde{x} \cdot \tilde{\xi}\} b(\tilde{x}, \tilde{\xi}) \hat{v}(\tilde{\xi}) d\tilde{\xi}.$$

Given a pseudo-differential operator $b(\tilde{x}, (1/i)\partial/\partial\tilde{x})$, this operator has the symbol $\sigma(b(\tilde{x}, (1/i)\partial/\partial\tilde{x})) = b(\tilde{x}, \tilde{\xi})$. One of the basic facts of the theory which we shall use is that if $a(\tilde{x}, \partial/\partial\tilde{x}) \in \text{OP}(S^{m_1})$ and $b(\tilde{x}, \partial/\partial\tilde{x}) \in \text{OP}(S^{m_2})$, then the composition $a \circ b \in S^{m_1 + m_2}$ and, furthermore, $\sigma(a \circ b)$ has the asymptotic expansion as $|\tilde{\xi}| \rightarrow \infty$ given by

$$(A.3) \quad \sigma(a \circ b) \sim \sum_{|\alpha| \geq 0} \frac{(-i)^{|\alpha|}}{\alpha!} \frac{\partial^\alpha}{\partial \tilde{\xi}^\alpha} a(\tilde{x}, \tilde{\xi}) \cdot \frac{\partial^\alpha}{\partial \tilde{x}^\alpha} b(\tilde{x}, \tilde{\xi}).$$

Radiation boundary conditions on the wall $x = a$. The key idea which we use to construct approximate radiation boundary conditions is a variable coefficient factorization procedure analogous to the frozen coefficient factorization (2.6). Below we shall derive an explicit special case of Lemma 1 on page 27 of [8]. This lemma allows one to factor the operator \mathcal{L} in the form

$$(A.4) \quad \mathcal{L} = \left(\frac{\partial}{\partial x} - \lambda_+ \left(x, \frac{1}{i} \frac{\partial}{\partial t}, \frac{1}{i} \frac{\partial}{\partial y} \right) \right) \left(\frac{\partial}{\partial x} - \lambda_- \left(x, \frac{1}{i} \frac{\partial}{\partial t}, \frac{1}{i} \frac{\partial}{\partial y} \right) \right) + (\text{smooth error}),$$

where $\lambda_{\pm}(x, (1/i) \partial/\partial t, (1/i) \partial/\partial y) \in \text{OP}(S^1)$ and the symbol of λ_{\pm} has the asymptotic expansion as $|\xi| \rightarrow \infty$ given by

$$(A.5) \quad \lambda_{\pm}(x, \xi, \omega) \sim \sum_{j=-1}^{\infty} \lambda_{\pm}^{-j}(x, \xi, \omega)$$

with $\lambda_{\pm}^{-j} \in S^{-j}$. As we shall see, in such a factorization the leading terms $\lambda_{\pm}^1(x, \xi, \omega)$ are determined by the frozen coefficient factorization

$$(A.6) \quad \lambda_{\pm}^1 = \pm i \xi \nu(x) \left(1 - \frac{\omega^2}{\xi^2 \nu^2(x)} \right)^{1/2}.$$

By applying Theorems 1 and 2 of [7], one verifies that, when \mathcal{L} acts on functions v defined for $x \leq a$, the asymptotic theoretical radiation boundary condition is given by

$$(A.7) \quad \left(\frac{\partial}{\partial x} - \lambda \left(x, \frac{1}{i} \frac{\partial}{\partial t}, \frac{1}{i} \frac{\partial}{\partial y} \right) \right) v \Big|_{x=a} = 0.$$

Using (A.5), one observes that

$$(A.8) \quad \left(\frac{\partial}{\partial x} - \sum_{j=-1}^R \lambda_{\pm}^{-j} \left(x, \frac{1}{i} \frac{\partial}{\partial t}, \frac{1}{i} \frac{\partial}{\partial y} \right) \right) v \Big|_{x=a} = 0$$

represents an “ $(R+1)$ -order” radiation boundary condition since it is asymptotic to (A.7) to the order $(|\xi|)^{R-1}$. For simplicity in exposition and for the applications needed in this paper, we set $R = 1$. Thus, to satisfy (A.4) to order $|\xi|^{-1}$, we need to choose λ_{\pm}^j , $j = 1, 0, -1$, so that

$$\sigma \left(\mathcal{L} - \left[\left(\frac{\partial}{\partial x} - \left(\lambda_+^1 + \lambda_+^0 + \lambda_+^{-1} \right) \right) \left(\frac{\partial}{\partial x} - \left(\lambda_-^1 + \lambda_-^0 + \lambda_-^{-1} \right) \right) \right] \right) \in S^{-1}.$$

We choose λ_{\pm}^1 as given in formula (A.6), in order that the terms of order $O(|\xi|^2)$ vanish. The terms of order $O(|\xi|)$, $O(1)$, respectively, must also vanish and this requires that

$$(A.9) \quad \begin{aligned} \left(-\frac{\partial}{\partial x} \lambda_{-}^1\right) + \lambda_{+}^0 \lambda_{-}^1 + \lambda_{+}^1 \lambda_{-}^0 &= 0 \quad \text{for } O(|\xi|), \\ \left(-\frac{\partial}{\partial x} \lambda_{-}^0\right) + \lambda_{+}^1 \lambda_{-}^{-1} + \lambda_{+}^0 \lambda_{-}^0 + \lambda_{+}^{-1} \lambda_{-}^1 &= 0 \quad \text{for } O(1). \end{aligned}$$

Necessarily we must take $\lambda_{+}^1 = -\lambda_{-}^1$ to avoid cross terms and we use (A.6) to compute the following formulae:

$$(A.10) \quad \begin{aligned} \lambda_{-}^1 &= -i\xi\nu(x) \left(1 - \frac{\omega^2}{\xi^2 \nu^2(x)}\right)^{1/2}, \\ \lambda_{-}^0 &= -\frac{1}{2} \frac{\partial \lambda_{-}^1 / \partial x}{\lambda_{-}^1}, \\ \lambda_{-}^{-1} &= -\frac{1}{2} \frac{\partial \lambda_{-}^0 / \partial x + (\lambda_{-}^0)^2}{\lambda_{-}^1}. \end{aligned}$$

By summarizing these calculations, we have

PROPOSITION A.1. *The approximate second-order theoretical radiating boundary condition for the operator \mathcal{L} in (A.1) acting on functions u defined in $x \leq a$ is given by*

$$(A.11) \quad \left(\frac{\partial}{\partial x} - \sum_{i=-1}^1 \lambda_{-}^i \left(x, \frac{1}{i} \frac{\partial}{\partial t}, \frac{1}{i} \frac{\partial}{\partial y}\right)\right) u \Big|_{x=a} = 0,$$

where the symbols λ_{-}^i are calculated explicitly from (A.10) given $\nu(x)$, an arbitrary index of refraction. The second-order local boundary condition analogous to \mathcal{B}_2 in Section 1 is given by

$$(A.12) \quad \left(\frac{\partial^2}{\partial x \partial t} + \nu \frac{\partial^2}{\partial t^2} - \frac{1}{2\nu} \frac{\partial^2}{\partial y^2} + \frac{\nu_x}{2\nu} \frac{\partial}{\partial t} + \frac{\nu_{xx}}{4\nu^2} - \frac{3\nu_x^2}{8\nu^3}\right) u \Big|_{x=a} = 0.$$

Radiation boundary conditions on the wall $y = b$. Next we repeat similar calculations on the wall $y = b$ and design theoretical radiation boundary conditions when \mathcal{L} acts on functions v defined for $y \leq b$. Again we shall factor \mathcal{L} within a smooth error as

$$(A.13) \quad \mathcal{L} \cong \left(\frac{\partial}{\partial y} - \lambda_{+} \left(x, \frac{1}{i} \frac{\partial}{\partial t}, \frac{1}{i} \frac{\partial}{\partial x}\right)\right) \left(\frac{\partial}{\partial y} - \lambda_{-} \left(x, \frac{1}{i} \frac{\partial}{\partial t}, \frac{\partial}{\partial x}\right)\right),$$

where we use the correspondence $i\theta \leftrightarrow \partial/\partial x$ under the Fourier transform. Given a factorization as in (A.13), the approximate theoretical radiation boundary condition is given by

$$\left(\frac{\partial}{\partial y} - \lambda_- \left(x, \frac{1}{i} \frac{\partial}{\partial t}, \frac{1}{i} \frac{\partial}{\partial x} \right) \right) v \Big|_{y=b} = 0.$$

As in the above, we only calculate the second-order theoretical radiation boundary condition; thus we need to choose $\lambda_+^i \in \text{OP}(S^i)$ so that

$$(A.14) \quad \sigma \left(\mathcal{L} - \left[\left(\frac{\partial}{\partial y} - (\lambda_+^1 + \lambda_+^0 + \lambda_+^{-1}) \right) \left(\frac{\partial}{\partial y} - (\lambda_-^1 + \lambda_-^0 + \lambda_-^{-1}) \right) \right] \right) \in S^{-1}.$$

According to (A.3),

$$\sigma(\lambda_+^1 \circ \lambda_-^1) - \left(\lambda_+^1 \lambda_-^1 - i \frac{\partial \lambda_+^1}{\partial \theta} \frac{\partial \lambda_-^1}{\partial x} - \frac{1}{2} \frac{\partial^2 \lambda_+^1}{\partial \theta^2} \frac{\partial^2 \lambda_-^1}{\partial x^2} \right) \in S^{-1},$$

and

$$\sigma(\lambda_+^1 \circ \lambda_-^0) - \left(\lambda_+^1 \lambda_-^0 - i \frac{\partial \lambda_+^1}{\partial \theta} \frac{\partial \lambda_-^0}{\partial x} \right) \in S^{-1},$$

$$\sigma(\lambda_+^0 \circ \lambda_-^1) - \left(\lambda_+^0 \lambda_-^1 - i \frac{\partial \lambda_+^0}{\partial \theta} \frac{\partial \lambda_-^1}{\partial x} \right) \in S^{-1}.$$

Condition (A.13) forces λ_+^1 to satisfy

$$(A.15) \quad \lambda_{\pm}^1 = \pm i\xi\nu(x) \left(1 - \frac{\theta^2}{\xi^2 \nu^2(x)} \right)^{1/2}$$

and also $\lambda_-^1 = -\lambda_+^1$.

Collecting the terms in (A.14) with $O(|\xi|)$ and $O(1)$, respectively, we obtain

$$(-i) \frac{\partial \lambda_+^1}{\partial \theta} \frac{\partial \lambda_-^1}{\partial x} + \lambda_+^1 \lambda_-^0 + \lambda_+^0 \lambda_-^1 = 0,$$

$$(-\frac{1}{2}) \frac{\partial^2 \lambda_+^1}{\partial \theta^2} \frac{\partial^2 \lambda_-^1}{\partial x^2} - i \left(\frac{\partial \lambda_+^0}{\partial \theta} \frac{\partial \lambda_-^1}{\partial x} + \frac{\partial \lambda_+^1}{\partial \theta} \frac{\partial \lambda_-^0}{\partial x} \right) + \lambda_+^1 \lambda_-^{-1} + \lambda_-^1 \lambda_+^{-1} = 0,$$

so that the following formulae for λ_{\pm}^i result:

$$(A.16) \quad \begin{aligned} \lambda_+^1 &= -i\xi\nu(x) \left(1 - \frac{\theta^2}{\xi^2 \nu^2(x)} \right)^{1/2}, \\ \lambda_-^0 &= \frac{i(\partial \lambda_+^1 / \partial \theta)(\partial \lambda_-^1 / \partial x)}{2\lambda_-^1}, \\ \lambda_-^{-1} &= \frac{\frac{1}{2} \frac{\partial^2 \lambda_-^1}{\partial \theta^2} \frac{\partial^2 \lambda_-^1}{\partial x^2} + i \left(\frac{\partial \lambda_-^0}{\partial \theta} \frac{\partial \lambda_-^1}{\partial x} + \frac{\partial \lambda_-^1}{\partial \theta} \frac{\partial \lambda_-^0}{\partial x} \right)}{2\lambda_-^1}. \end{aligned}$$

We have

PROPOSITION A.2. *The second-order theoretical radiation boundary condition on the wall $y = b$ for the operator \mathcal{L} acting on functions v defined for $v \leq b$ is given by*

$$(A.17) \quad \left(\frac{\partial}{\partial y} - \sum_{i=-1}^1 \lambda_i^1 \left(x, \frac{1}{i} \frac{\partial}{\partial t}, \frac{1}{i} \frac{\partial}{\partial x} \right) \right) u \Big|_{y=b} = 0,$$

where λ_i^1 are calculated by the formulae (A.16). The second-order local boundary condition which involves at most second-order derivatives is given by

$$(A.18) \quad \left(\frac{\partial^2}{\partial y \partial t} + \nu \frac{\partial^2}{\partial t^2} - \frac{1}{2\nu} \frac{\partial^2}{\partial x^2} + \frac{\nu_x}{2\nu^2} \frac{\partial}{\partial x} + \frac{\nu_{xx}}{4\nu^2} - \frac{\nu_x^2}{4\nu^3} \right) u \Big|_{y=b} = 0.$$

Appendix B

Finite Difference Formulae for Radiation Boundary Conditions

The function $u(x, y, t)$ is approximated for $x \leq a$, $y \leq b$ by u_{jk}^n on the grid (x_j, y_k, t^n) , $x_j = j\Delta x$, $y_k = k\Delta y$, $t^n = n\Delta t$, $j \leq J$, $k \leq K$. Approximative radiation boundary conditions are given for $j = J$ and $k = K$.

The acoustic wave equation with variable index of refraction, $\nu(x)$.
Approximation of (A.12) at $x_j = a$:

$$(B.1) \quad \begin{aligned} D_-^x D_0^t u_{jk}^n + \left(\frac{1}{2} \nu D_+^t D_-^t + \frac{\nu_x}{4\nu} D_0^t \right) (u_{j-1,k}^n + u_{jk}^n) \\ + \left(-\frac{1}{4\nu} D_+^y D_-^y + \frac{\nu_{xx}}{8\nu^2} - \frac{3\nu_x^2}{16\nu^3} \right) (u_{j-1,k}^{n+1} + u_{jk}^{n-1}) = 0. \end{aligned}$$

Here

$$\nu = \nu(x_{j-1/2}), \quad \nu_x = \frac{\partial}{\partial x} \nu(x_{j-1/2}), \quad \nu_{xx} = \frac{\partial^2}{\partial x^2} \nu(x_{j-1/2}).$$

The derivatives of ν can of course also be approximated by divided differences.

Approximation of (A.18) at $y_k = b$:

$$(B.2) \quad \begin{aligned} D_-^y D_0^t u_{jk}^n + \left(\frac{1}{2} \nu D_+^t D_-^t + \frac{\nu_x}{4\nu^2} D_0^x \right) (u_{j,K-1}^n + u_{jk}^n) \\ + \left(-\frac{1}{4\nu} D_+^x D_-^x + \frac{\nu_{xx}}{8\nu^2} - \frac{\nu_x^2}{8\nu^3} \right) (u_{j,K-1}^{n+1} + u_{jk}^{n-1}) = 0. \end{aligned}$$

For the first-order methods with only first derivatives the difference approximations are

$$(B.3) \quad \frac{1}{2}D_-^x(u_{jk}^n + u_{jk}^{n+1}) + \frac{1}{2}\nu D_+^t(u_{jk}^n + u_{j-1,k}^n) + \frac{\nu_x}{4\nu}(u_{jk}^n + u_{j-1,k}^{n+1}) = 0 \quad \text{at } x_j = a,$$

$$(B.4) \quad \frac{1}{2}D_-^y(u_{jk}^n + u_{jk}^{n+1}) + \frac{1}{2}\nu D_+^t(u_{jk}^n + u_{j,k-1}^n) = 0 \quad \text{at } y_k = b.$$

The elastic wave equation. Approximation of (3.20) at $x_j = a$:

$$(B.5) \quad D_-^x D_0^t u_{jk}^n + \frac{1}{2}A_0 D_+^t D_-^t(u_{j-1,k}^n + u_{jk}^n) + \frac{1}{2}\tilde{A}_1 D_0^y D_+^t(u_{j-1,k}^n + u_{jk}^{n-1}) + \frac{1}{2}\tilde{A}_2 D_+^y D_-^y(u_{j-1,k}^{n+1} + u_{jk}^{n-1}) = 0.$$

Here the matrix A_0 is defined in (3.16), \tilde{A}_1 and \tilde{A}_2 are defined in (3.21).

Approximation at $y_k = b$: The analogue of (3.20) for the boundary $y = b$ can be written as

$$(B.6) \quad \left(\frac{\partial^2}{\partial y \partial t} + A^{(0)} \frac{\partial^2}{\partial t^2} + A^{(1)} \frac{\partial^2}{\partial x \partial t} + A^{(2)} \frac{\partial^2}{\partial x^2} \right) v \Big|_{y=b} = 0,$$

where

$$(B.7) \quad A^{(0)} = \begin{pmatrix} 1/\sqrt{d_2} & 0 \\ 0 & 1/\sqrt{d_1} \end{pmatrix}, \quad A^{(1)} = (\sqrt{d_2} - \sqrt{d_1}) \begin{pmatrix} 0 & 1/\sqrt{d_2} \\ 1/\sqrt{d_1} & 0 \end{pmatrix},$$

$$A^{(2)} = \begin{pmatrix} \frac{1}{2}\sqrt{d_2} - \sqrt{d_1} & 0 \\ 0 & \frac{1}{2}\sqrt{d_1} - \sqrt{d_2} \end{pmatrix}.$$

The difference approximation is

$$(B.8) \quad D_-^y D_0^t u_{jk}^n + \frac{1}{2}A^{(0)} D_+^t D_-^t(u_{j,k-1}^n + u_{jk}^n) + \frac{1}{2}A^{(1)} D_0^x D_+^t(u_{j,k-1}^n + u_{jk}^{n-1}) + \frac{1}{2}A^{(2)} D_+^x D_-^x(u_{j,k-1}^{n+1} + u_{jk}^{n-1}) = 0.$$

The approximation at the corner $x_j = a$, $y_k = b$ for the acoustic wave equation:

$$(B.9) \quad (D^x + D^y)(u_{jk}^n + u_{jk}^{n+1}) + \frac{2}{3}\sqrt{2}\nu D_+^t(u_{j,k-1}^n + u_{j-1,k}^n + u_{jk}^n) = 0$$

for $(j, k) = (J, K-1)$, $(J-1, K)$, (J, K) . A similar formula can be used at corners for the elastic case (see [2]).

All the difference equations presented in this appendix are explicit and second-order accurate.

Bibliography

- [1] Boore, D., *Finite difference methods for seismic wave propagation in heterogeneous materials*, *Methods of Computational Physics (Seismology)*, Academic, New York, 1972, Vol. 115 pp. 1-37.
- [2] Clayton, R., and Engquist, B., *Absorbing boundary conditions for acoustic and elastic wave equations*, *Bull. Seismol. Soc. Amer.* 67(6), 1977, pp. 1529-1540
- [3] Elvius, T., and Sundstrom, A., *Computationally efficient schemes and boundary conditions for a fine mesh barotropic model based on the shallow water equations*, *Tellus* 25, 1973, pp. 132-156.
- [4] Engquist, B., and Majda, A., *Absorbing boundary conditions for the numerical simulation of waves*, *Math. Comput.* 31 (139), 1977, pp. 629-651.
- [5] Kelly, K. R., Alford, R. M., Treitel, S., and Ward, R. W., *Applications of finite difference methods to exploration seismology*, *Proceedings of the Royal Irish Academy Conference on Numerical Analysis*, Academic, New York, 1974, pp. 57-76.
- [6] Kreiss, H.-O., *Initial boundary value problems for hyperbolic systems*, *Commun. Pure Appl. Math.* 23, 1970, pp. 277-298.
- [7] Majda, A., and Osher, S., *Reflection of singularities at the boundary*, *Commun. Pure Appl. Math.* 28, 1975, pp. 479-499.
- [8] Nirenberg, L., *Lectures on Linear Partial Differential Equations*, C. B. M. S. Regional Conf. Ser. in Math., No. 17, Amer. Math. Soc., Providence, R. I., 1973
- [9] Roache, P. J., *Computational Fluid Dynamics*, Hermose Press, Albuquerque, N. M., 1972.
- [10] Sirovich, L., *Techniques of Asymptotic Analysis*, Springer-Verlag, New York, 1971, Applied Math Sciences No. 2.

Received June, 1978.